

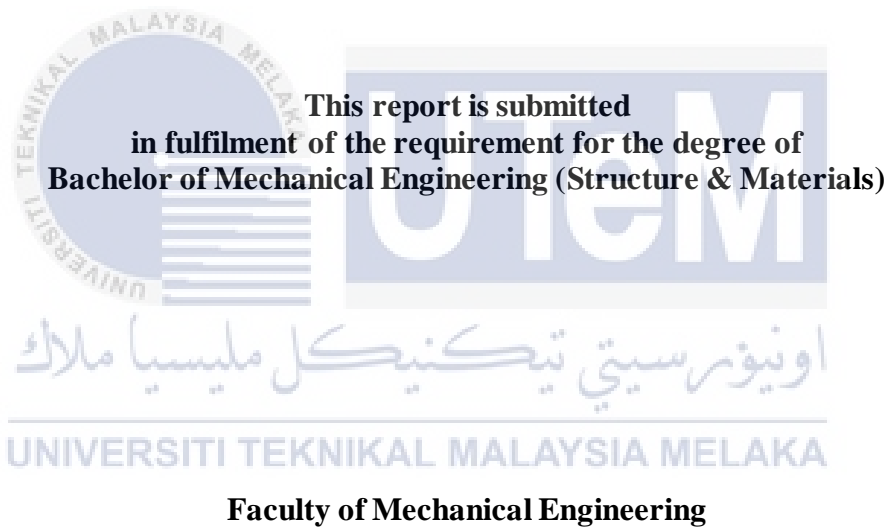
**PARAMETRIC STUDY ON THE DEVELOPMENT OF SUBSTITUTE  
MATERIALS FOR STRETCHABLE CONDUCTIVE INK (SCI) AS A  
FUNCTION OF CONDUCTIVE FILLER LOADING**



**UNIVERSITI TEKNIKAL MALAYSIA MELAKA**

**PARAMETRIC STUDY ON THE DEVELOPMENT OF SUBSTITUTE  
MATERIALS FOR STRETCHABLE CONDUCTIVE INK (SCI) AS A  
FUNCTION OF CONDUCTIVE FILLER LOADING**

**SHHRUL AZIM BIN MAT YUSOFF**



**UNIVERSITI TEKNIKAL MALAYSIA MELAKA**

**JANUARY 2022**

## DECLARATION

I declare that this project report entitled "Parametric study on the development of substitute materials for Stretchable Conductive Ink (SCI) as a function of conductive filler loading" is the result of my own work except as cited in the references

Signature : .....

Name : .....

Date : .....



اونيورسيتي تيكنيكل مليسيا ملاك

UNIVERSITI TEKNIKAL MALAYSIA MELAKA

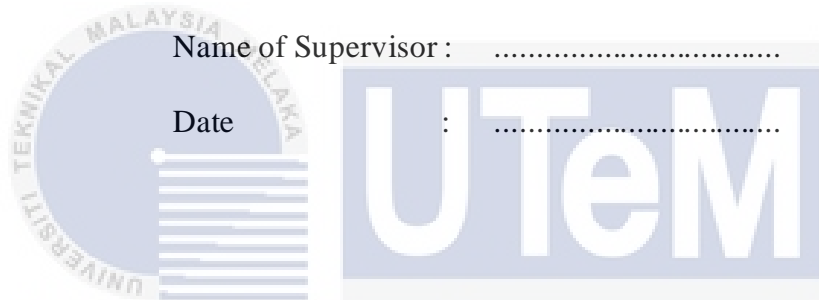
## APPROVAL

I hereby declare that I have read this project report, and in my opinion, this report is sufficient in terms of scope and quality for the award of the degree of Bachelor of Mechanical Engineering.

Signature : .....

Name of Supervisor : .....

Date : .....



اونيورسيتي تيكنيكل مليسيا ملاك  
UNIVERSITI TEKNIKAL MALAYSIA MELAKA

## DEDICATION

To my beloved mother and father



## ABSTRACT

In this study, a 15  $\mu\text{m}$  Graphene Nanoplatelets (GNP) is used as a conductive filler in a Poly (3,4-ethylene dioxythiophene) Polystyrene Sulfonate (PEDOT: PSS) polymer matrix in formulating the stretchable conductive ink (SCI) in which the Thermoplastic polyurethane (TPU) is used as a substrate. The SCI system sets the GNP filler loading to 5, 7.5 and 10 wt.%. The parametric study includes establishing the optimum temperature, mixing time and mixing speed in the Thinky Mixer centrifugal mixer followed by curing in the oven. The ratio between materials used in the SCI formulation was calculated using the Rule of Mixture (ROM) for composites. The optimum process parameters established in this study are at a curing temperature of 60°C for 15 minutes. The optimum mixing time and speed in the Thinky Mixer is 10 minutes at a mixing speed of 400 rpm. Based on visual observation during the formulation of the SCI, to overcome the presence of brittleness of the cured SCI ink and the bubble formed in the blending of PEDOT: PSS with the GNP filler, surfactants were introduced. Dimethyl sulfoxide (DMSO), Mono Ethylene Glycol (MEG), and Triton-X100 were included in the optimum SCI formulation before the electrical characterization of the SCI. Based on the electrical characterization via a Four-point probe as per ASTM F390, an optimum average sheet resistivity is attained at a GNP filler loading of 10 wt.%, with a value of  $3.97 \pm 0.46 \Omega/\text{sq.}$ , which yield in conductivity of 2518.9 S/m. Surface morphology of the SCI reveal traces of void formation at the lowest GNP filler loading of 5 wt.%, and better homogeneity is evident at increasing GNP filler loading. The preliminary results on the newly formulated SCI using these materials combination suggest a promising potential of the ink for uses in flexible electronics applications.

UNIVERSITI TEKNIKAL MALAYSIA MELAKA

## ABSTRAK

Dalam kajian ini, 15  $\mu\text{m}$  Graphene Nanoplatelets (GNP) digunakan sebagai pengisi konduktif dalam matriks polimer Poli (3,4-etilena dioksitiofen) Polistirena Sulfonat (PEDOT: PSS) dalam formulasi dakwat konduktif boleh renggang (SCI) di mana Poliuretana termoplastik (TPU) digunakan sebagai substrat. Sistem SCI ini menggunakan 5, 7.5 dan 10 wt.% muatan bahan pengisi GNP. Kajian parameter di dalam projek penyelidikan ini mengambil kira suhu optimum, masa pencampuran dan kelajuan pencampuran dalam pengadun emparan *Thinky Mixer* diikuti dengan pengerasan di dalam ketuhar. Nisbah antara bahan yang digunakan dalam formulasi SCI dikira menggunakan Peraturan Campuran (ROM) untuk komposit. Parameter proses optimum yang ditetapkan dalam kajian ini adalah pada suhu pengerasan  $60^{\circ}\text{C}$  selama 15 minit. Masa dan kelajuan adunan optimum dalam pengadun emparan *Thinky Mixer* ialah 10 minit pada kelajuan adunan 400 rpm. Berdasarkan pemerhatian visual semasa formulasi SCI, untuk mengatasi masalah kerapuhan dakwat SCI yang telah dikeraskan dan gelembung udara yang terbentuk di dalam adunan PEDOT: PSS dengan pengisi GNP, surfaktan telah diperkenalkan. Dimetil sulfoksida (DMSO), Mono Ethylene Glycol (MEG), dan Triton-X100 dimasukkan dalam formulasi optimum SCI sebelum pencirian sifat elektrik. Berdasarkan pencirian elektrik melalui kuar empat mata dengan merujuk kepada ASTM F390, kerintangan kepingan purata optimum dicapai pada muatan pengisi GNP sebanyak 10 wt.%, dengan nilai  $3.97 \pm 0.46 \Omega/\text{sq.}$ , yang menghasilkan kekonduksian sebanyak 2518.9 S/m. Morfologi permukaan SCI mendedahkan kesan pembentukan lompong pada muatan pengisi GNP terendah iaitu 5 wt. %, dan kehomogenan yang lebih baik dapat dilihat pada peningkatan pemuatan pengisi GNP. Berdasarkan penemuan awal daripada kajian bahan SCI dengan formulasi baru yang menggunakan gabungan bahan-bahan yang dipilih ini menunjukkan bahawa dakwat ini mempunyai potensi untuk kegunaan di dalam aplikasi elektronik fleksibel.

## ACKNOWLEDGEMENT

Firstly, I would like to take this opportunity to express my sincere acknowledgement to my supervisor, Dr. Siti Hajar Binti Sheikh Md. Fadzullah from the Faculty of Mechanical Engineering of Universiti Teknikal Malaysia Melaka (UTeM) for her valuable time and energy and her supervision, support, and encouragement to complete this project.

I would also like to express my deepest gratitude to Zuraimi bin Ramle, a PhD student from the Faculty of Mechanical Engineering, for his advice, consultations and suggestions throughout this project, which gave me a clear vision of how the research project should be conducted. Special thanks to my senior, Solehah Binti Jasmee, for providing me with the equipment and guidance for contact angle test and my friend, Asyraf, for their commitment and co-operation in completing this project. Special thanks to the Faculty of Mechanical Engineering, Universiti Teknikal Malaysia Melaka (UTeM) and JABIE Circuit Sdn. Bhd. for the financial support throughout this project.



## TABLE OF CONTENTS

|  |      |
|--|------|
| DECLARATION.....   | ii   |
| APPROVAL.....  | iii  |
| DEDICATION .....   | iv   |
| ABSTRACT.....  | v    |
| ABSTRAK.....   | vi   |
| ACKNOWLEDGEMENT.....                                       | vii  |
| TABLE OF CONTENTS .....                                    | viii |
| LIST OF TABLES.....  | xi   |
| LIST OF FIGURES .....                                      | xii  |
| LIST OF ABBREVIATIONS.....                                 | xiv  |
| LIST OF SYMBOLS .....                                      | xv   |
| CHAPTER 1 .....  | 1    |
| INTRODUCTION.....  | 1    |
| 1.1 Background.....  | 1    |
| 1.2 Problem Statement.....                                 | 2    |
| 1.3 Objective .....  | 3    |
| 1.4 Scope of Project.....                                  | 4    |
| 1.5 General Methodology.....                               | 4    |
| CHAPTER 2 .....  | 8    |
| LITERATURE REVIEW .....                                    | 8    |
| 2.1 Introduction .....                                     | 8    |
| 2.2 Stretchable Conductive Inks .....                      | 8    |
| 2.3 Conductive fillers in Stretchable Conductive Inks..... | 10   |
| 2.3.1 Carbon Fillers.....                                  | 10   |
| 2.3.2 Metal fillers.....                                   | 13   |
| 2.4.3 Ceramic Filler.....                                  | 13   |
| 2.4 Type of Polymer binder.....                            | 15   |
| 2.4.1 PEDOT: PSS.....                                      | 15   |
| 2.4.2 Epoxies.....   | 18   |
| 2.5 Substrate.....   | 20   |

|             |   |    |
|-------------|---|----|
| 2.5.1       | Thermoplastic Polyurethane (TPU) .....  | 23 |
| 2.5.2       | Polyethylene Terephthalate (PET) .....  | 23 |
| 2.6         | The Important of Surfactant in stretchable Conductive Inks .....                | 23 |
| 2.6.1       | Dimethyl sulfoxide (DMSO).....  | 23 |
| 2.6.2       | Mono Ethylene Glycol (MEG).....   | 24 |
| 2.6.3       | Triton-X-100 .....  | 25 |
| 2.7         | Processing of the SCI .....   | 26 |
| 2.7.1       | Optimization of The Sci of Graphene Nanoplate (GNP 5 $\mu$ m and 15 $\mu$ m) 27 |    |
| 2.8         | Properties of Stretchable Conductive Ink.....                                   | 27 |
| 2.8.1       | Electrical Resistivity.....   | 28 |
| 2.8.2       | Mechanical Properties .....   | 29 |
| 2.8.2.1     | Stretchability Test.....  | 30 |
| 2.8.2.2     | Scratch Test on Graphene Nanoplate .....  | 31 |
| CHAPTER 3   | .....   | 37 |
| METHODOLOGY | .....   | 37 |
| 3.1         | Overview.....   | 37 |
| 3.2         | Flow Chart.....   | 38 |
| 3.3         | Raw Materials.....  | 39 |
| 3.3.1       | Polymer binder.....   | 39 |
| 3.3.2       | filler .....  | 41 |
| 3.3.3       | Surfactant.....   | 41 |
| 3.3.3.1     | Dimethyl Sulfoxide (DMSO).....  | 42 |
| 3.3.3.2     | Mono Ethylene Glycol (MEG) .....  | 43 |
| 3.3.3.3     | Triton-X-100 .....  | 44 |
| 3.4         | Substrate .....   | 45 |
| 3.4.1       | Thermoplastic polyurethane (TPU).....   | 45 |
| 3.5         | Formulation of SCI .....  | 46 |
| 3.5.1       | The GNP filled PEDOT: PSS Formulation .....                                     | 46 |
| 3.5.2       | GNP- filled PEDOT: PSS and Surfactant Formulation .....                         | 48 |
| 3.6         | Characterization of The SCI .....   | 53 |
| 3.6.1       | Electrical Property Using a Four-Point Probe.....                               | 53 |
| 3.6.2       | Bulk Resistivity of The SCI .....   | 55 |
| 3.6.3       | Scanning Electron Microscope.....   | 55 |

|   |    |
|---|----|
| CHAPTER 4 .....   | 57 |
| RESULTS AND DISCUSSION .....  | 57 |
| 4.1 Introduction .....  | 57 |
| 4.2 Parametric Study Of The GNP-Filled PEDOT: PSS SCI Formulation ..                        | 58 |
| 4.2.1 Effect Of Processing Parameters (Mixing Time And Speed) .....                         | 58 |
| 4.2.2 The Effect of Surfactant Used in GNPs And PEDOT: PSS<br>Formulation .....             | 61 |
| 4.3 Effect of Mixing Speed and Mixing Time Of GNP Filled PEDOT: PSS<br>With Surfactant..... | 62 |
| 4.4 The Bulk Resistivity Test of GNP filled PEDOT: PSS Surfactant.....                      | 63 |
| 4.5 Surface Morphology of The GNP filled PEDOT: PSS: Surfactant SCI.....                    | 64 |
| CHAPTER 5 .....   | 67 |
| CONCLUSION AND RECOMMENDATION .....   | 67 |
| 5.1 Conclusion.....   | 67 |
| 5.2 Recommendation for Future Works .....   | 68 |
| REFERENCES .....  | 70 |



اونيورسيتي تيكنيكل مليسيا ملاك

UNIVERSITI TEKNIKAL MALAYSIA MELAKA

## LIST OF TABLES

|   |    |
|---|----|
| Table 1.1 The research planning and activities for PSM I.....                 | 6  |
| Table 1.2 The research planning and activities for PSM II.....                | 7  |
| Table 2.1 The particle size of conductive ink for the three widths.....       | 22 |
| Table 2.2 Designation and properties of investigation .....                   | 26 |
| Table 3.1 Selected material specification for PEDOT: PSS with 1.3 wt. %.....  | 40 |
| Table 3.2 Specification of Graphene nanoplatelets conductive filler .....     | 41 |
| Table 3.3 The physical and chemical properties of MEG used in this study..... | 43 |
| Table 3.4 Specification of the TPU substrate. ....                            | 45 |
| Table 3.5 Hybrid Graphene- PEDOT: PSS formulation.....                        | 50 |
| Table 3.6 Detail information on the specific contents of the PEDOT: PSS ..... | 51 |
| Table 4.1 The Sheet Resistivity and Conductivity of the SCI.....              | 59 |
| Table 4.2 The sheet resistivity and contact angle of the SCI .....            | 60 |
| Table 4.3 Sheet Resistivity and Conductivity of the SCI .....                 | 62 |
| Table 4.4 The Average Bulk Resistivity of the SCI.....                        | 63 |
| Table 4.5 SEM micrograph showing the GNP filler .....                         | 65 |
| Table 4.6 SEM micrograph showing the GNP .....                                | 66 |

## LIST OF FIGURES

|   |    |
|---|----|
| Figure 2.1 Structure of Graphene in graphitic forms.....                              | 11 |
| Figure 2.2 AFM images of PEDOT PSS(Yang et al., 2020).....                            | 16 |
| Figure 2.3 An illustration of the (a) electron transport in a PEDOT: PSS .....        | 17 |
| Figure 2.4 Reaction process in producing bisphenol-A epoxy (Yi et al., 2010).....     | 18 |
| Figure 2.5 Bulk Resistivity of the test patterns using PET and TPU substrates .....   | 21 |
| Figure 2.6 Sheet Resistivity of carbon on TPU and PET.....                            | 22 |
| Figure 2.7 Comparison of electrical resistivity of GNP .....                          | 29 |
| Figure 2. 8 Properties of GNP composites using the melt-extrusion process.....        | 31 |
| Figure 2.9 Normal displacement (Shokrieh et al., 2013).....                           | 34 |
| Figure 2.10 An AFM image from the scratch test on GNP-filled .....                    | 35 |
| Figure 2.11 The cross-section scratch profiles of GNP-filled.....                     | 36 |
| Figure 3.1 Flow chart of the methodology .....  | 38 |
| Figure 3.2 Sigma Aldrich PEDOT: PSS.....  | 39 |
| Figure 3.3 The chemical structure of Sigma Aldrich PEDOT: PSS .....                   | 40 |
| Figure 3.4 Dimethyl Sulfoxide (DMSO) used in this study.....                          | 42 |
| Figure 3.5 The chemical structure of Dimethyl Sulfoxide (DMSO) .....                  | 42 |
| Figure 3.6 Mono Ethylene Glycol (MEG) used in this study.....                         | 43 |
| Figure 3.7 Triton X-100 used in this study.....                                       | 44 |
| Figure 3.8 The Triton X-100 chemical structure (SIGMA-ALDRICH, 2022e).....            | 44 |
| Figure 3.9 The chemical structure of Thermoplastic polyurethane (TPU).....            | 46 |
| Figure 3.10 Bubble formation found following solution mixing of the SCI .....         | 48 |
| Figure 3.11 The steps in GNP-filled PEDOT: PSS SCI .....                              | 52 |
| Figure 3.12 A JANDEL In-Line Four-Point Probe .....                                   | 53 |
| Figure 3.13 An example of the SCI printed onto a TPU substrate .....                  | 54 |
| Figure 3.14 Experimental set up for the Bulk resistivity test on the SCI sample ..... | 55 |
| Figure 3.15 A Scanning Electron Microscope from JEOL Model .....                      | 56 |

Figure 4. 1 The sheet resistivity of the SCI at specified processing parameters with varying GNP filler loading..... 61

Figure 4.2 Sheet resistivity and the corresponding conductivity of the SCI with varying mixing parameters and GNP filler loading..... 63



## LIST OF ABBREVIATIONS

|       |                                   |
|-------|-----------------------------------|
| 3D    | Three Dimensional                 |
| CNT   | Carbon nanotubes                  |
| CVD   | Chemical vapor decomposition      |
| ECA   | Electrically conductive adhesive  |
| ICA   | Isotropically Conductive Adhesive |
| MWCNT | Multiwall carbon nanotubes        |
| NCA   | Non-Conductive Adhesive           |
| PDMS  | Polydimethylsiloxane              |
| SEM   | Scanning Electron Microscope      |
| SWCNT | Single wall carbon nanotubes      |
| TPU   | Thermoplastic polyurethane        |
| UV    | Ultra violet                      |
| GNP   | Graphene Nanoplatelets            |
| GCN   | Graphene Carbon Nanoplatelets     |
| DMSO  | Dimethyl sulfoxide                |
| MEG   | Mono Ethylene Glycol              |
| X-100 | Triton X-100                      |

## LIST OF SYMBOLS

|                    |   |                     |
|--------------------|---|---------------------|
| $\mu$              | = | Micro               |
| $^{\circ}\text{C}$ | = | Degree Celsius      |
| k                  | = | Kelvin              |
| $\Omega$           | = | Ohm                 |
| sq                 | = | Square              |
| $T_g$              | = | Glass temperature   |
| g                  | = | Gram                |
| m                  | = | Meter               |
| nm                 | = | Nanometer           |
| $\mu\text{m}$      | = | Micrometer          |
| L                  | = | Length              |
| OD                 | = | Outer diameter      |
| $V_m$              | = | Volume of matrix    |
| $V_f$              | = | Volume of fiber     |
| $V_c$              | = | Volume of composite |
| wt%                | = | Weight percentage   |
| mm                 | = | Milimeter           |
| $\tau$             | = | Shear               |
| F                  | = | Force               |
| A                  | = | Area                |
| R                  | = | Resistance          |



# CHAPTER 1

## INTRODUCTION

### 1.1 Background

Due to complex and expensive procedures, today's printed circuit board (PCB) producers pay relatively high costs. Stretchable conductive inks (SCI) have grown in popularity due to their high flexibility and expendability while keeping excellent conductivity. Due to the exceptional properties of nanocarbon-based materials (graphene and CNT), the fillers in SCI have to be moved from metallic to nanocarbon-based materials (graphene and CNT). However, there is a scarcity of good data on specific industrial-based applications, which has resulted in a lack of industry interest in exploring this technology. Furthermore, understanding the thermomechanical influence of nanocarbon-based materials in SCI, both on their functioning and dependability, is critical, and this knowledge is currently lacking. The usefulness, performance, and durability of replacing metal fillers with nanocarbon-based materials have yet to be thoroughly investigated. The process of creating SCI materials is arduous and time-consuming. (As a result, this research aims to find the best materials composition and ideal parameters for producing the SCI (A. S. Ashikin et al., 2019)

TPU is a high-performance thermoplastic elastomer used in coatings, adhesives, reaction injection moulding, fibers, foams, thermoplastic elastomers, and composites. TPU is a highly elastic material that can withstand up to 1000

percent strains. According to Merilampi et al. (2009), many factors affect the sheet resistance of conductive ink, including curing ink conditions, ink viscosity, and filler content of ink. The consequences on the flexible and elastic substrate, on the other hand, have yet to be thoroughly understood. (A. S. Ashikin et al., 2013)

## 1.2 Problem Statement

Stretchable conductive inks (SCI) have grown in popularity due to their high flexibility and expendability while keeping excellent conductivity. To solve these issues, numerous conductive fillers are utilized in the printed electronics market, including gold, platinum, carbon nanotube, silver nanoparticles, and organic conductive polymers (Ashikin et al., 2013). Furthermore, graphene can be employed to reduce the manufacturing cost of PCB technology.

The board is physically frail and can easily break when pushed under extreme pressure. Low manufacturing costs, long-term durability, environmentally sustainable production processes, recycling, lower energy consumption and improved efficiency, and electronic integration as part of other structures are all essential new electronic features. Copper, aluminium, and nickel are less expensive alternatives because of the high materials cost (Ashikin et al., 2013). However, one of these materials' drawbacks is that it is easily oxidized in the air, generating an insulating barrier on their surface. The SCI provides a one-of-a-kind solution for integrating electronics into apparel, accessories, and medical devices. The ink can be utilized to produce a thin, stretchy formfitting circuit in wearable devices that allows for both

comfort and freedom. Because of its multiplexing mobility, one of the critical issues in wearable chemical sensors in real-life scenarios is that it can create poor deformations of wearable equipment, including power supplies and sensors.

The samples in this thesis were printed to reduce total production time and cost-effective with higher quantities because printing is a low-cost and quick means of manufacturing multiple samples. As demonstrated in a recent work, screen printing is one approach for creating conductive ink patterns directly on flat or even irregularly shaped and curved surfaces. Electronic circuits are printed using various technologies, including gravure printing, inkjet printing, and flexographic printing. (A. A. Ashikin et al.,2019)

### 1.3 Objective

The objectives of this project are as follows:

- i. To develop a newly formulated SCI with varying GNP filler loading using optimum process parameters
- ii. To characterize the electrical and mechanical properties of the newly formulated SCI.

## 1.4 Scope of Project

The scopes of this project are:

- I. Formulating new nanocarbon-based SCI using different weight percent.
- II. Fabrication of the SCI with optimized formulation using a centrifugal mixer machine
- III. Electrical characterization of the SCI using a four-point probe iv. Mechanical characterization of the SCI using a customized jig for stretchability study
- IV. Morphological analysis of the SCI using a Scanning Electron Microscope (SEM)

## 1.5 General Methodology

In general, the following research activities will be sought throughout this semester for

PSM I, as listed below: -

1. Literature review

Journals, articles, or any published materials related to the project will be reviewed and analyzed.

2. Design of experiment (DOE)

DOE is a powerful data collection and analysis tool used in various experimental situations. It allows multiple input factors to be manipulated, determining their effect on the desired output. In this

study, a specific DOE software tool will be used to optimize the newly formulated SCI

### 3. Stretchable conductive ink (SCI)

Conductive filler is a functional material that enables the ink film to have better electrical, which possesses good conductivity after stretching and folding. (Kim et al., 2020)

Table 1.1 demonstrates the research planning and activities for PSM I, while in Table 1.2, the research activities planned for PSMII. For this semester, upon confirmation of the chosen topic, a literature review is done to understand the research related to the project. Later, in Week 7, the progress report is due for submission.

From the established literature, the design of experimental work will be carried out using a specific tool. Next, formulation and fabrication of the SCI's samples will be carried out, and the analysis of the preliminary experiment will be made and analyzed. Finally, a report will be submitted, and the primary literature and preliminary results will be presented in the PSM 1 seminar.

Table 1.1 The research planning and activities for PSM I

| Activities/Week         | 1 | 2 | 3 | 4 | 5 | 6 | 7 | 8 | 9 | 10 | 11 | 12 | 13 | 14 | 15 |
|-------------------------|---|---|---|---|---|---|---|---|---|----|----|----|----|----|----|
| Research title review   |   |   |   |   |   |   |   |   |   |    |    |    |    |    |    |
| Literature review       |   |   |   |   |   |   |   |   |   |    |    |    |    |    |    |
| Design of experiment    |   |   |   |   |   |   |   |   |   |    |    |    |    |    |    |
| Sample fabrication      |   |   |   |   |   |   |   |   |   |    |    |    |    |    |    |
| Testing/Data collection |   |   |   |   |   |   |   |   |   |    |    |    |    |    |    |
| Data analysis           |   |   |   |   |   |   |   |   |   |    |    |    |    |    |    |
| Report writing          |   |   |   |   |   |   |   |   |   |    |    |    |    |    |    |
| Report submission       |   |   |   |   |   |   |   |   |   |    |    |    |    |    |    |
| PSM presentation        |   |   |   |   |   |   |   |   |   |    |    |    |    |    |    |

Table 1.2 The research planning and activities for PSM II

| Activities/Week         | 1 | 2 | 3 | 4 | 5 | 6 | 7 | 8 | 9 | 10 | 11 | 12 | 13 | 14 | 15 |
|-------------------------|---|---|---|---|---|---|---|---|---|----|----|----|----|----|----|
| Literature review       |   |   |   |   |   |   |   |   |   |    |    |    |    |    |    |
| Design of experiment    |   |   |   |   |   |   |   |   |   |    |    |    |    |    |    |
| Sample fabrication      |   |   |   |   |   |   |   |   |   |    |    |    |    |    |    |
| Testing/Data collection |   |   |   |   |   |   |   |   |   |    |    |    |    |    |    |
| Data analysis           |   |   |   |   |   |   |   |   |   |    |    |    |    |    |    |
| Report writing          |   |   |   |   |   |   |   |   |   |    |    |    |    |    |    |
| Report submission       |   |   |   |   |   |   |   |   |   |    |    |    |    |    |    |
| PSM presentation        |   |   |   |   |   |   |   |   |   |    |    |    |    |    |    |

## CHAPTER 2

### LITERATURE REVIEW

#### 2.1 Introduction

This chapter provides an overview of connection materials, electrically conductive adhesives, polymers, fillers, carbon nanotubes, and their mechanical, electrical, and thermal properties based on past research.

#### 2.2 Stretchable Conductive Inks

Stretchable conductive inks (SCI) have grown in popularity due to their high flexibility and expendability while keeping excellent conductivity. Due to the exceptional properties of nanocarbon-based materials (graphene and CNT), the fillers in SCI have to be moved from metallic to nanocarbon-based materials (graphene and CNT). However, there is a scarcity of good data on specific industrial-based applications, which has stifled industry enthusiasm in pursuing this technology for their products (Merilampi et al., 2009). Furthermore, understanding the thermomechanical impact of nanocarbon-based materials in SCI is critical for their functioning and reliability, which is currently lacking. The usefulness, performance, and durability of replacing metal fillers with nanocarbon-based materials have not been thoroughly investigated. The process of creating SCI materials is arduous and time-consuming. As a result, this research aims to find the best materials composition and ideal parameters for producing the SCI.



Printed circuits, organic light-emitting diodes, radio-frequency identification tags, and battery test stripes are all made with conductive inks in the printed electronics industry. The flexibility, lightweight design, and lower prices are the key benefits of such items. Conductive inks are made up of a variety of complicated compositions. The conductive component is the most significant, and it can be made of metal or carbon particles and conductive polymers. The conductive particles are dispersed in resins, giving mechanical and adhesive qualities. Solvents are used to dissolve the resins and manage the ink's rheological qualities, while additives are utilized to change the ink's processability and functional properties (Nguyen et al., 2020).

Screen printing, gravure printing, flexography, and inkjet printing have all treated conductive inks. Previous studies looked at how conductive inks performed on different substrates such as paper, glass, and polymer films. However, printability and functional qualities of conductive inks on anticorrosive primer coatings have yet to be studied. As a result, the primary goal of this research is to assess the printability and characteristics of various conductive inks on a variety of primer coatings for use in the printed electronics sector. Furthermore, any relationships between the substrate's structure and the printed inks' functional qualities should be assessed (2019, Mendez-Rossal & Wallner).

### 2.3 Conductive fillers in Stretchable Conductive Inks

To make the polymer matrix conductive, fillers are added to electrically conductive glue. Silver (Ag), gold (Au), Copper (Cu), Nickel (Ni), and Carbon are a few examples of filler. However, copper and nickel deteriorate easily and decrease conductivity and reliability, so fillers are not typically employed. (Ashikin et al., 2020)

The size and form of the conductive filler are also crucial factors in the characteristics of ECA. Therefore, to minimize the filler loading volume fraction and obtain the appropriate electrical characteristics, a more significant aspect ratio of the conductive filler is required to lower the percolation threshold. Furthermore, higher mechanical characteristics can be attained by reducing the percolation threshold decreasing filler loading.

#### 2.3.1 Carbon Fillers

Graphene is one of the fascinating materials being studied right now, not just for its academic value but also for its future applications. It's a two-dimensional substance made up of carbon atom layers. Graphene, which includes zero-dimensional fullerenes, one-dimensional carbon nanotubes, and three-dimensional graphite, is the mother of all graphitic forms (Fig. 1). Carbon nanotubes and graphene have very different electronic and Raman spectra and other features, including electrical conductivity and mechanical strength. (Raheem, 2018).

Graphene is a two-dimensional substance with a single layer; however, graphene samples with two layers (bi-layer) and more than two but less than 10 layers (few-layer graphene) are also of interest. Most graphene physical

research has been done on single-layer sheets created using micro-mechanical cleavage techniques.

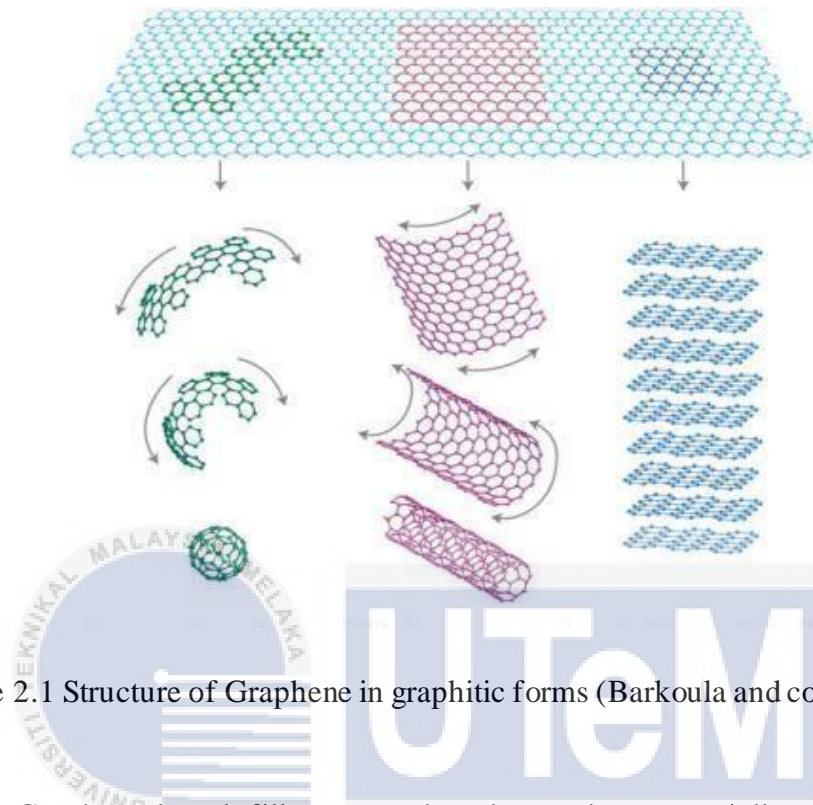


Figure 2.1 Structure of Graphene in graphitic forms (Barkoula and colleagues, 2008)

Graphene-based fillers are thought to be potentially significant multifunctional nanofillers because they have outstanding electrical and thermal properties similar to carbon nanotubes (CNT) and a two-dimensional shape similar to silica-alumina layered clays. Furthermore, producing thin graphene nanoplatelets made up of many layers of graphene sheets is straightforward and inexpensive. Intercalation, where both electron-donor agents and electron acceptors can be intercalated in between graphene layers; exfoliation, where a large amount of heat is applied to expand the intercalated agent; and pulverization, where the exfoliated graphite is down-sized to smaller platelets, are the three steps involved in fabricating these nanoplatelets from natural graphite.

The compounding procedure affects the distribution, separation, and orientation of the nanofillers in a nanocomposite, which can change their distribution, separation, and orientation. Melt compounding, in which high-density polyethylene (HDPE) and exfoliated graphite are mixed in a Brabender mixer or twin-screw extrusion; solution mixing, in which a solvent is used to dissolve the polymer and then the graphite is added and dispersed in situ polymerization, in which monomers are usually intercalated in between graphite layers (Barkoula and colleagues, 2008)

Carbon nanoparticles work well as filler materials as well. Carbon nanotubes, graphene, and graphene oxide (GO) are among the carbon nanomaterials being investigated for this purpose. Graphene, in particular, is attracting a lot of interest due to its exceptional physical qualities, including tensile strength [10], lubricating properties [11], and thermal conductivity.

In the study by Kim et al. (2017), multi-walled carbon nanotubes (MWNTs), exfoliated graphite nanoplatelets (xGnPs), and graphene oxide were the nanocarbon filler materials examined (GO). It was argued that the most effective filler type after optimizing the nanocarbon content. A 1:1 combination of MWNT and GO was tested as a novel filler material. They focused in quantifying dispersibility and determining the significance of the examined mechanical qualities. PA66/NC materials could be used to make high-strength mechanical components. It was argued that these materials are particularly well-suited to applications in which the material will be subjected to high friction. These materials can also be employed as conductive flexible films, supercapacitor flexible electrodes, and bioengineering applications. (2017, Kim et al.)

### 2.3.2 Metal fillers

Since the polymer matrices that link to the conductive fillers are dielectric materials, the electrical conductivity of ECA is provided by the conductive fillers. There are two types of conductive filler for ECA: metal and non-metal material. Furthermore, the conductivity performance of ECA must be as high as feasible, and the conductive fillers loading must be equal to or greater than the percolation threshold to be effective (Yi et al., 2010).

In metals, the electrical conductivity is produced by the movement of electrically charged particles inside the substance. Electric current may flow through a metal because its valence electrons can travel freely, which allows the current to flow. As the electrons moved, they knocked each other about and sent an electric charge between them. Silver, gold, and copper are metals with low electrical resistance and high electrical conductivity performance. Conversely, silver, gold, and copper are examples of metals with low valence electrons (Bell, 2017). Li, Lumpp, Andrews, and Jacques (2008) found that the high loading of conductive metal filler necessary to obtain adequate electrical conductivity in ECA resulted in a decrease in the strength to weight ratio and dependability of the ECA.

### 2.4.3 Ceramic Filler

Ceramic material has been getting a lot of attention from material science in the last few years because it has a lot of good things, like a high melting temperature, a high hardness, a high modulus of elasticity, chemical resistance, poor conductivity, and low ductility. In ceramic materials, bonding is usually a mix of ionic and covalent, but it can also have a Van-der-Waals or metallic part in it, too. Ceramic fillers are

another vital type of conductive filler. They have better thermal conductivity and good electrical insulation, which is why they are essential.

Boron Nitride (BN) and other ceramic fillers make things stronger. SiC, TiN, TiC, TiB<sub>2</sub> and TiB are some fillers. These types of ceramic fillers have caught the attention of scientists and engineers who want to use them in their research projects. Overall, it said that the epoxy/BN composite-impregnated coil outperformed the other coils in cooling, over-current, and repeated cooling tests. As a result, the epoxy/BN composite may be the best way to make very stable superconducting rotating machines much more reliable (Jeong et al., 2016).

Nanoscale ceramic materials have been used to study how epoxy-based adhesives' electro-conductivity is affected by these materials. Researchers and their associates, for example, studied the electrical conductivity of ceramic and metallic nanofluids. According to the experiment's findings, adding a surfactant to nanofluids increases their stability while decreasing their electrical conductivity. Increasing surface area and electrophoretic mobility of alumina nanoparticles lead to an increase in the electrical conductivity of water-based nanofluids. In addition, nanofluids with low ionic strength exhibit an increase in electrical conductivity, whereas nanofluids with high ionic strength indicate a reduction in electrical conductivity. It is because of variances in the particle's surface (Sarojini et al., 2013).

## 2.4 Type of Polymer binder

Polymer binders are the essential ingredient in cementitious waterproofing sealing slurries, as they offer substrate adherence, water tightness (permeability), and flexibility.

### 2.4.1 PEDOT: PSS

PEDOT: PSS has been intensively studied in recent years, with many research efforts devoted to improving these flexible features through molecular or structural design. The most frequent way to modify such conductive polymers' properties is to blend and mix various polymers and fillers into PEDOT: PSS; however, a corresponding review paper is still missing, notably on stretchable electronics thermoelectric applications. (Yang et al., 2020) The main focus is the electrical conductivity, stretchability, and thermoelectric properties of these PEDOT: PSS blends and composites. PEDOT: PSS (poly (3,4- ethylene dioxythiophene): poly (styrene sulfonate)) is a polyelectrolyte composed of negatively charged insulating PSS and positively charged electrically conducting PEDOT. PSS polymer anions can stabilize conjugated polymer cations (Ham and colleagues, 2012).

PEDOT: PSS is still in the development stage, despite its excellent electrical conductivity, low sheet resistance, outstanding transparency, and thermoelectric properties, especially for applications like conductive, flexible, or even stretchable, wearable electronic devices.

Blends and composites based on PEDOT: PSS with various components. We mainly focused on the impacts of different compatibility and distribution

states on the tensile and conductivity characteristics of these materials to further analyze the relationship between the structure and properties of these blends. Although PEDOT: PSS films are potential prospects for flexible organic light-emitting diodes, transparent electrodes, and electrostatic coatings, the majority of applications rely on their mechanical as well as electrical qualities (Figure 2.2).

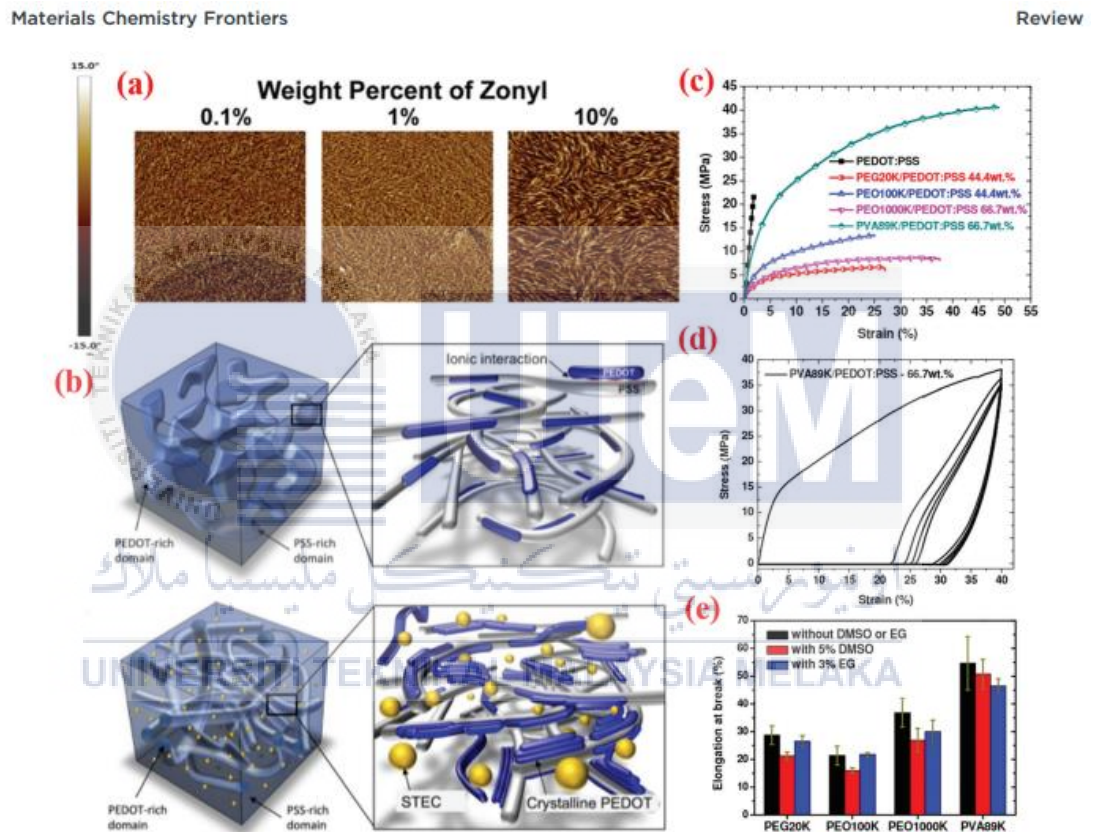


Figure 2.2 AFM images of PEDOT PSS(Yang et al., 2020)

PEDOT: PSS films partially expand, decreasing PSS molecular chains' hydrogen bonds and increasing the free volume of twisted PEDOT and PSS molecular chains, allowing the chain segment to relax and endure mechanical damage and tensile strain fully.

83 Crystalline soft polymer blends exhibit a faster rise in conductivity than blends with an insulating amorphous soft polymer (PEO).



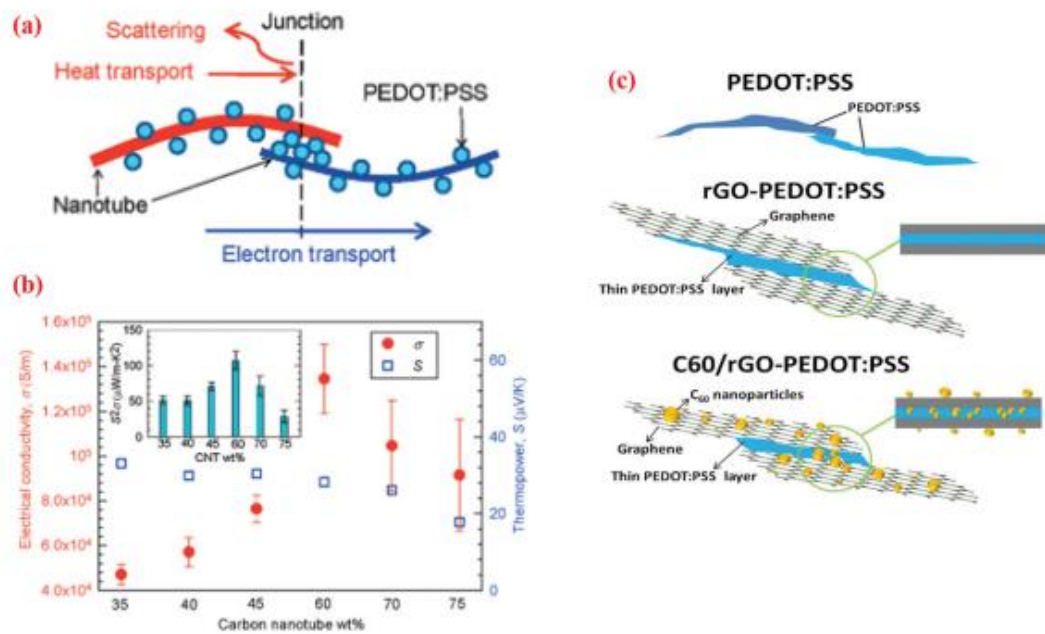


Figure 2.3 An illustration of the (a) electron transport in a PEDOT: PSS-CNT junctions in the composites; (b) the electrical conductivity of the hybrid composites and in (c) illustration of the different types of hybrid composites systems studied (Yang et al., 2020)

First and foremost, in the case of flexible PEDOT: PSS blends, increased stretchability is frequently associated with reduced electrical conductivity, despite the adoption of a secondary doping approach. Because of the incompatibility of the elastomer and PEDOT: PSS, Bulk PEDOT: PSS conductors are typically challenging to produce, especially for immiscible polymer/PEDOT: PSS mixtures. There is limited research on developing hierarchical structures or nanoconfined PEDOT: PSS in elastic matrixes to form conductive routes, aside from composite fibres, because the finite-size effect and the interfacial impact can result in unusual thermodynamic and kinetic properties. More careful management of the processing approach and interfacial contact is anticipated to lead to more complex phase morphologies with improved characteristics. Yang et al. (Yang et al., 2020)

## 2.4.2 Epoxies

Epoxide resins are a type of polymeric substance that contains more than one three-membered ring, such as epoxy, epoxide, oxirane, or ethoxyline. Epoxies are a type of polymer that has a wide range of applications, including metal can coatings, automobile primers, printed circuit boards, semiconductor encapsulants, adhesives, and aerospace composites.

Epoxies are the preferred polymeric materials in the electronic industry because they provide excellent resistance to chemical and corrosion, outstanding physical and electrical qualities, good adhesion, thermal insulation, minimal shrinkage, and a fair cost of material for the industry. Figure 2.1 illustrates the process of preparing epoxies, which is typically based on the chemical bisphenol-A, which is transformed into bisphenol-A epoxy after interacting with epichlorohydrin (Yi et al., 2010).

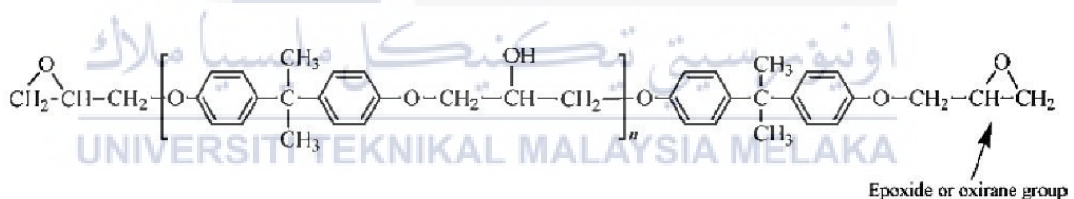


Figure 2.4 Reaction process in producing bisphenol-A epoxy (Yi et al., 2010).

The repletion number might range from zero to around 30 (hard solid) depending on the liquid. It is the reactant ratio between bisphenol-A and epichlorohydrin that determines the viscosity of epoxy, and this ratio is between bisphenol-A and epichlorohydrin. Several types of epoxy curing agents are available, including amines, anhydrides, dicyandiamides, melamine formaldehydes, urea formaldehydes, phenol formaldehyde and catalytic curing agents, with anhydride and amines being the most commonly employed (Yi et al., 2010).

The curing agents are selected in accordance with the curing condition, application procedures, pot life requirement, and physical features that have been defined. The curing agents influence the viscosity and reactivity of epoxy formulations while also allowing the process to decide the degree of cross-linking and the formation of chemical bonds in the cured epoxy system, among other things. Occasionally, an accelerator such as a tertiary amine is employed to speed up the sluggish chemical reaction between anhydrides and epoxies in certain circumstances. The terms "Novolacs" and "Resole" refer to two different types of epoxies. Novolac epoxy is a formaldehyde acid-catalyzed epoxy polymer that exhibits high temperature and chemical resistance due to a methylene bridge connecting the phenolic group inside the epoxy. Novolac epoxy is available in a variety of colours. Resole epoxy, a base-catalyzed phenol-formaldehyde resin, has excellent chemical resistance and cures at a high temperature, making it a good choice for outdoor applications (Yi et al., 2010). When it comes to device encapsulation and moulding compounds, high purity epoxy resins are used since the polymers minimize the quantity of chloride and mobile ions present. Furthermore, to reduce the polymer's thermal coefficient of expansion (CTE), tiny, well-controlled spheres of crystalline silica with a fine distribution have to be mixed into the polymer systems as fillers. Incorporating a tiny amount of elastomeric materials into stiff epoxy results in an increase in epoxy toughness while simultaneously lowering the epoxy elastic modulus and thermal stress. Because of its low-stress properties, the low-stress polymer is well suited for various applications such as conductive adhesives and moulding compounds (Yi et al., 2010).

## 2.5 Substrate

The total conductivity is controlled by conductive filler materials, filler surface resistance, polymer matrix conductivity, and hopping conductivity. However, the conductivity of the polymer matrix is modest compared to the conductivity of filler materials and thus can be ignored. Merilampi and Mohammed (2009) reported the conductivity and resistivity of the polymer composite. Conductive particles agglomerate together to form a 3D conductive connection (Wan Abdul Rahman, 2017).

The Bulk resistivity of printed conductive ink on PET and TPU substrates with three distinct trace widths of 1, 2, and 3-mm is shown in Figure 2.5. The resistance flow along the conductive ink is measured using bulk resistivity. All samples exhibit a similar pattern, with the bulk resistivity decreasing as the trace width grows. The electron route expands as the trace width widens. Carbon black, with particle sizes ranging from 30 to 50 nm, is an excellent material for making electrically conductive composites. Its particle size causes large particle aggregation, resulting in a vast network at low concentrations. The ink amount rises as the trace width increases, forming a more extensive network inside the ink. (Wan Abdul Rahman, 2017)

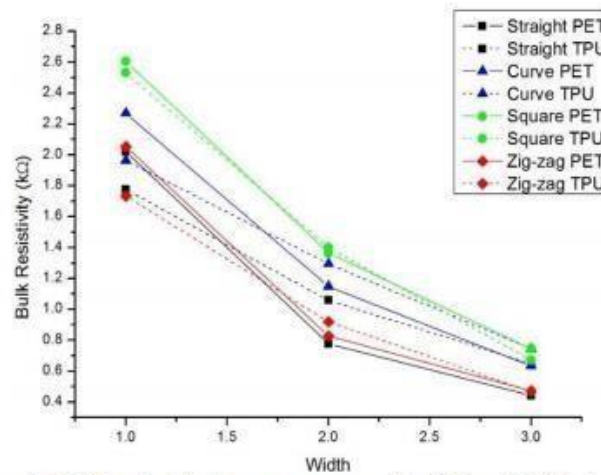


Figure 2.5 Bulk Resistivity of the test patterns using PET and TPU substrates (Wan Abdul Rahman, 2017)

Sheet resistivity for four patterns on PET and TPU substrates is shown in Figure 5, and all of the samples demonstrate a drop in sheet resistivity as the trace width increases. Due to its soft surface, conductive ink on the TPU substrate has a lower sheet resistivity than conductive ink on the PET substrate. As a result, the carbon black particles become closer, creating more conductive routes for electrons to travel from one particle to the next. Because the concentration of conductive filler increases with the broader trace, the sheet resistivity of the conductive ink lowers as the trace width grows. As the concentration of conductive filler grows, it creates electrical contact between the particles and improves the conductivity of conductive ink.

According to Merilampi (2009), conductive filler concentration increased conductivity because the charge carriers increased as the filler contact increased. The contact area between particles, on the other hand, can improve the resistance to constriction on the asperities contact.

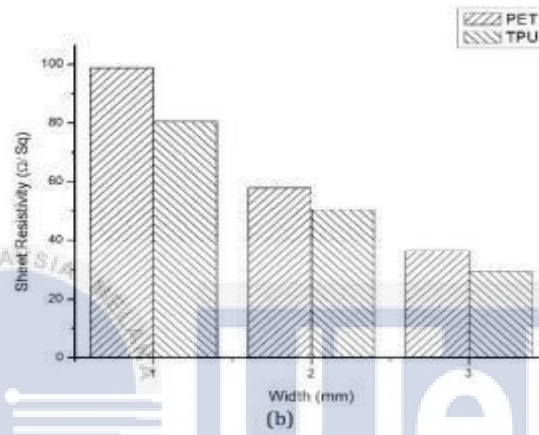
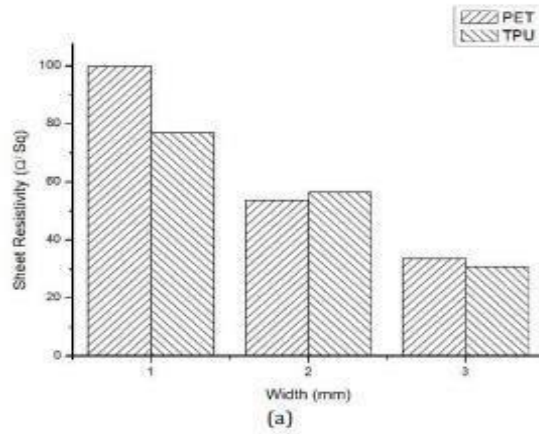


Figure 2.6 Sheet Resistivity of carbon on TPU and PET (Wan Abdul Rahman, 2017)

— Table 2.1 The particle size of conductive ink for the three widths  
 UNIVERSITI TEKNIKAL MALAYSIA MELAKA

|     | PET                          |                          |                          |                       | TPU                          |                          |                          |                       |
|-----|------------------------------|--------------------------|--------------------------|-----------------------|------------------------------|--------------------------|--------------------------|-----------------------|
|     | Average<br>( $\mu\text{m}$ ) | Min<br>( $\mu\text{m}$ ) | Max<br>( $\mu\text{m}$ ) | Standard<br>Deviation | Average<br>( $\mu\text{m}$ ) | Min<br>( $\mu\text{m}$ ) | Max<br>( $\mu\text{m}$ ) | Standard<br>Deviation |
| 1mm | 0.623                        | 0.244                    | 1.549                    | 0.388                 | 0.512                        | 0.161                    | 1.122                    | 0.266                 |
| 2mm | 0.511                        | 0.201                    | 1.006                    | 0.235                 | 0.225                        | 0.063                    | 0.419                    | 0.100                 |
| 3mm | 0.473                        | 0.165                    | 0.960                    | 0.230                 | 0.236                        | 0.133                    | 0.558                    | 0.109                 |

### **2.5.1 Thermoplastic Polyurethane (TPU)**

TPU, derived from one type of thermoplastic elastomer (TPE), was likewise used as the test pattern's substrate. TPU can be treated into a molten state and then solidified to reclaim its rubber-like characteristics. TPE is a co-polymeric material made up of hard and soft polymeric chains. Due to the substrate's stretchability and soft nature, conductive ink on the TPU substrate has a lower bulk resistance than conductive ink on the PET substrate, which is stiffer. (Wan Abdul Rahman, 2017)

### **2.5.2 Polyethylene Terephthalate (PET)**

PET was chosen as an ink substrate because of its flexibility, chemical resistance (save for alkalis), and mechanical features such as stiffness, low water absorption, strength while being affordable, and thin thickness. Furthermore, PET crystallinity ranges from amorphous to relatively high crystalline. (Wan Abdul Rahman, 2017). Figure 2.6 shows that ink traces on PET substrates with 1 mm width have higher Bulk resistivity than ink traces on TPU substrates for all four layouts.

## **2.6 The Important of Surfactant in stretchable Conductive Inks**

### **2.6.1 Dimethyl sulfoxide (DMSO)**

In addition to its potential to trigger cell fusion and differentiation, dimethyl sulfoxide (DMSO) also has the ability to increase the permeability of lipid membranes. It's also an excellent cryoprotectant to have on hand. A better understanding of how this molecule influences membrane structure and function would be essential in controlling the processes described above and devising chemical ways of enhancing

or limiting the absorption of physiologically active substances, particularly into or through the skin. One of the most common ways to use DMSO is for topical or transdermal drug delivery, where its ability to make the skin more permeable is used. Therefore, it would be essential to develop molecules that control how active molecules move through membranes.

DMSO's ability to change the permeability of membranes may also help it be a good cryo protectant. Because DMSO can quickly get inside cells, its primary role in cryopreservation is thought to be to keep ice from crystallizing inside cells. In the "slow cooling" cryopreservation method, ice forms in the extracellular space, making the remaining water more concentrated with solutes (Notman et al., 2006)

### **2.6.2 Mono Ethylene Glycol (MEG)**

As a result of the high volume of water that must be evaporated during the thermal recovery of mono ethylene glycol (MEG) from aqueous streams, this process is one of the most energy-intensive procedures in the industry. The employment of alternative technologies, such as liquid-liquid extraction, has the potential to reduce energy use. Mono ethyl glycol (MEG) is one of the most significant glycols in the chemical industry. It is widely employed as an antifreeze agent, polymer precursor, and preservative in the cosmetic business, among other things. MEG is created through the neutral hydrolysis of ethylene oxide in a laboratory setting.

Typically, a substantial amount of water is used to avoid the formation of by-products (e.g., diethylene glycol (DEG), tri ethylene glycol (TEG), and higher EG oligomers) throughout the process. As a result, alternative procedures that do not



involve water evaporation should be investigated since they have the potential to save significant quantities of energy (Garcia-Chavez et al., 2012).

### 2.6.3 Triton-X-100

It is a non-ionic surfactant in which the poly oxy methylene chains remain outside the core and move relatively freely in the solvent, allowing the micelles to remain stable in solution when the hydrocarbon part of the micelle is considered to be a liquid hydrocarbon. Triton-X-100 [p-(1,1,3,3-tetramethyl butyl) phenoxy poly (oxy ethylene) glycol] is a non-ionic surfactant in which the poly oxy methylene chains remain outside the core.

Surfactants are frequently utilized in various chemical formulations, and synergism can often be detected between the diverse compounds in the formulation. Here, synergism is defined as the state in which the qualities of a combination are superior to those that may be obtained by combining the constituent components individually. A mixed system containing both ionic surfactants and non-ionic surfactants is essential. TX-100 was obtained as a result of this. Water was deionized and then doubled distilled to remove impurities (El-Aila, 2009)

## 2.7 Processing of the SCI

In Table 2.3, the designation and properties of investigation on Graphite and PEDOT: PSS reported in past research by Mendez-Rossal & Wallner (2019) are listed. Solvent inks like graphite and silver are paste-like. The silver ink formulations had the most considerable conductive particle fraction, ranging from 60 to 70%. The PEDOT: PSS polymer ink was a gelatinous water-based ink with a low quantity of PEDOT. As a result, it was argued that the sheet resistance of the polymer ink was higher than that of the silver inks (Mendez-Rossal & Wallner, 2019)

Table 2.2 Designation and properties of investigation (Mendez-Rossal & Wallner, 2019)

| Ink ID | Type       | Type of solvent/ink | Conductive agent content (% m) | Sheet resistance (Ohm/sq.) |
|--------|------------|---------------------|--------------------------------|----------------------------|
| I_g    | Graphite   | Solvent/paste       | 16.5                           | Not provided               |
| I_ml   | Silver     | Solvent/paste       | 68.5                           | <0.001                     |
| I_m2   | Silver     | Solvent/paste       | 61                             | 0.007                      |
| I_p    | PEDOT: PSS | Water/gel           | 2.5                            | 400                        |

### 2.7.1 Optimization of The Sci of Graphene Nanoplate (GNP 5 $\mu\text{m}$ and 15 $\mu\text{m}$ )

The fabrication of graphene nanoplatelets, made up of many layers of graphene sheets, is relatively straightforward and inexpensive. Fabrication of these nanoplatelets from natural graphite usually involves three steps: (i) intercalation, in which both electron-donor and electron-acceptor agents are intercalated between graphene layers; (ii) exfoliation, in which a large amount of heat is applied to expand the intercalated agents; (iii) pulverization, in which the exfoliated graphite is down-sized to smaller platelets.

Exfoliated graphite nanoplatelets (GNP) can be manufactured via acid intercalation, microwave heating, and ultrasonic pulverization. This path can lead to cost-effective industrial-scale manufacturing (XG Sciences, East Lansing, MI). During manufacture, the lateral width of GNP nanoplatelets can be adjusted. Nanoplatelets are typically 5 and 15  $\mu\text{m}$  in diameter and designated as GNP-5, respectively. (Mendez-Rossal & Wallner, 2019)

### 2.8 Properties of Stretchable Conductive Ink

The GNP particles are homogeneously distributed in Bulk and separated by a polymer matrix. Mechanical properties benefit from this shape. The comparatively smooth surface shows a homogenous coating layer of GNP particles. A layer of graphite phase generated by coating forms the border between the left and right sides.

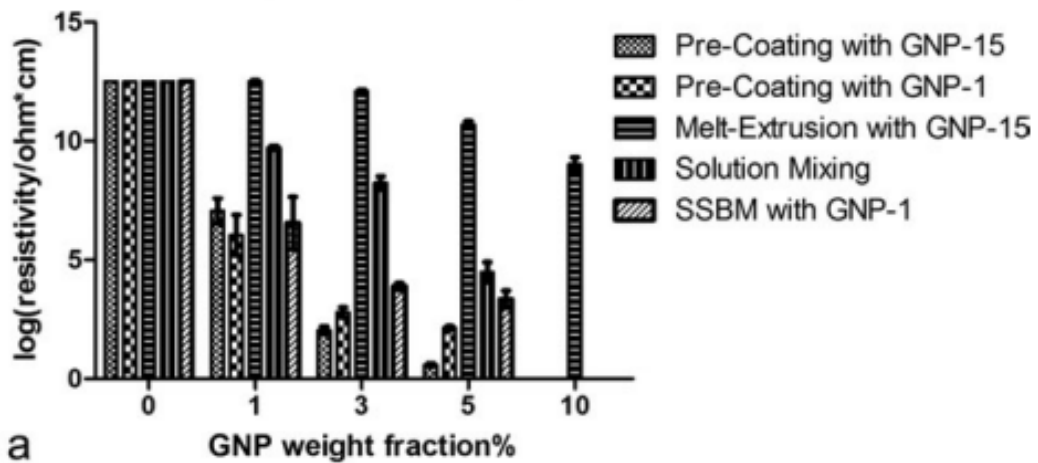
This approach produces high mechanical capabilities while simultaneously lowering the percolation threshold by generating a continuous GNP coating on the surface of a size reduced polymer powder with good

adherence. The SSBM method produced composites with a percolation threshold similar to pre-coating but with higher mechanical characteristics and without solvent. The GNP nanocomposites' morphology revealed the results of several compounding processes. Pre-coating and SSBM succeed in generating a continuous phase of the conductive GNP nanofillers. Still, melt-extrusion tends to cause discrete GNP phases by separating and lowering the size of the GNP particles. (Htwe et al., 2021)

### **2.8.1 Electrical Resistivity**

The electrical resistivity of the GNP composites reported by Barkoula et al. (2008) is shown in Figure 2.7 (Barkoula et al., 2008). Because of particle anisotropy and alignment during compression moulding, the resistivity in the in-plane direction is always lower than in the through-plane direction. The single sheet has a thickness of a few nanometres. A large sheet with several smaller platelets is adhering to it. The linked GNP particles created by the platelet-shaped nature could not be separated efficiently during extrusion, decreasing the amount of effective fillers (Barkoula et al., 2008)

Electrical Conductivity of GNP/PEI<sub>d</sub> Composites - In-Plane



Electrical Conductivity of GNP/PEI<sub>d</sub> Composites - Through-Plane

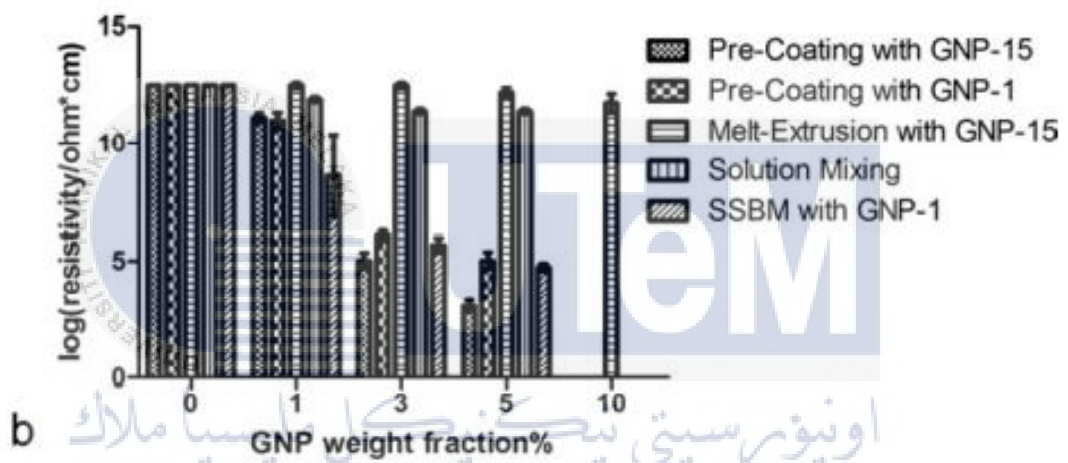


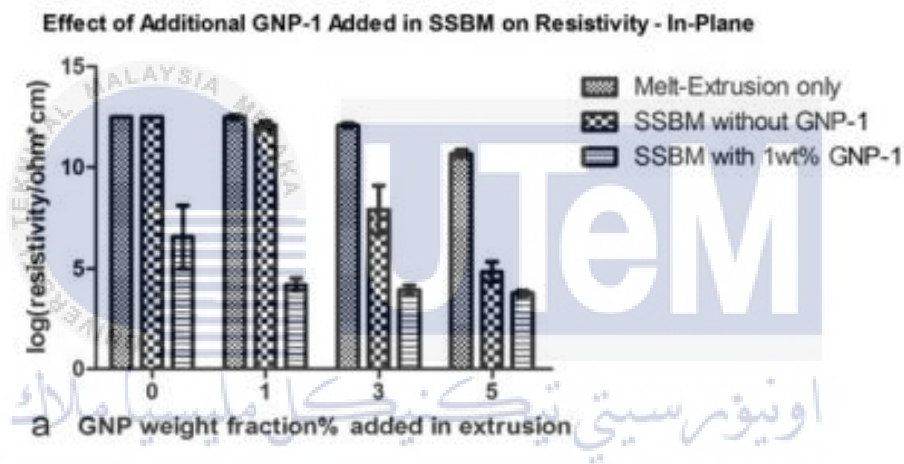
Figure 2.7 Comparison of electrical resistivity of GNP (Barkoula et al., 2008)

### 2.8.2 Mechanical Properties

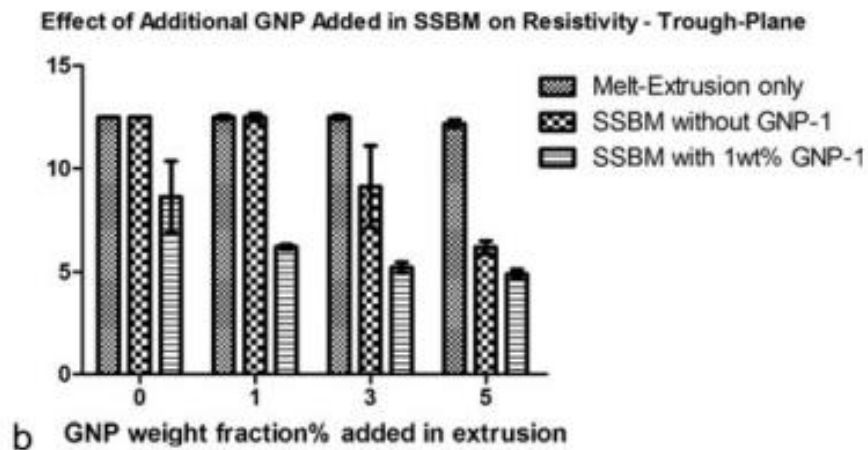
Mechanical properties are the physical characteristics that a material exhibits when applied. The modulus of the stretchability test and the scratch test are two examples of mechanical qualities.

### 2.8.2.1 Stretchability Test

Although melt-extrusion effectively distributes GNP particles to obtain excellent flexural characteristics, it is insufficient to prevent the particles from restacking. Electrical percolation in the nanocomposite can be achieved with highly modest GNP added in the SSBM process. The electrical resistance, flexural modulus, and strength of the composites produced by the two-step compounding technique combining melt extrusion and SSBM are shown in Figure 2.8 (Barkoula et al., 2008)



UNIVERSITI TEKNIKAL MALAYSIA MELAKA



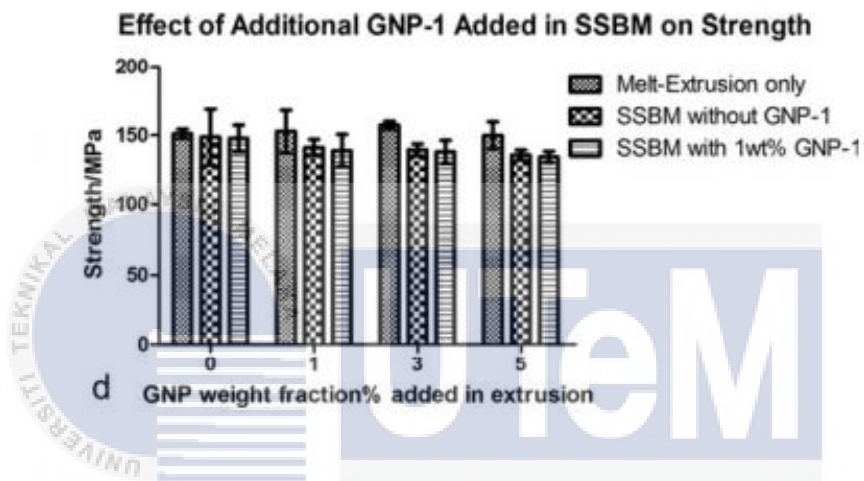
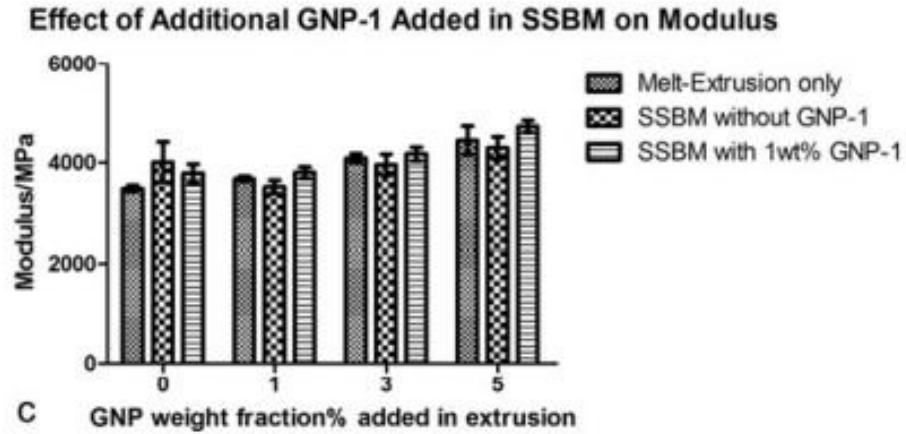
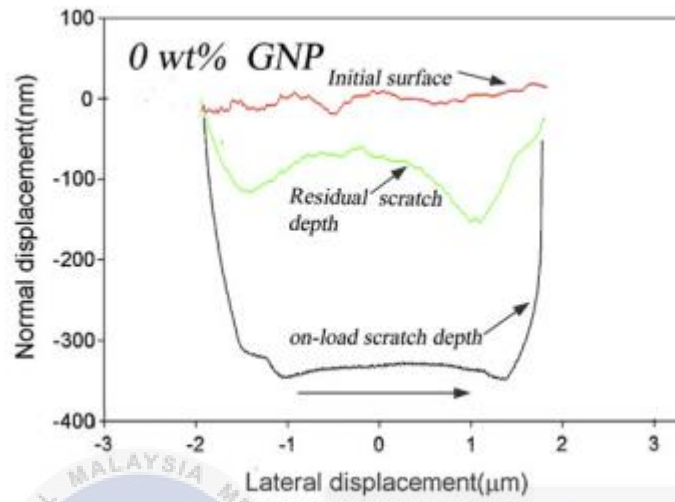


Figure 2. 8 Properties of GNP composites using the melt-extrusion process in terms of the (a) in-plane resistivity; (b) through-plane electrical resistivity; (c) flexural modulus and (d) flexural strength (Barkoula et al., 2008)

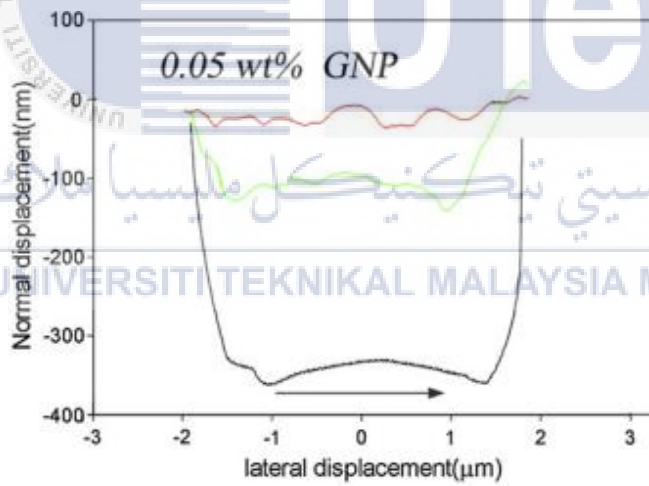
### 2.8.2.2 Scratch Test on Graphene Nanoplate

Scratch hardness is a valuable metric for determining relative scratch resistance. This method is extensively used to compare the scratch resistance of various materials. An analogy with indentation hardness has been used to establish scratch hardness ( $H_s$ ). The scratch hardness can be estimated with a Berkovich indenter using the following equation:  $F_N$  is the maximum normal force applied to the indenter during the nano-scratch test,  $A$  is the residual scratch groove area, and  $d$

is the residual scratch width. Scratch and normal hardness are plotted as functions of GNP content in **Figure 2.9**.

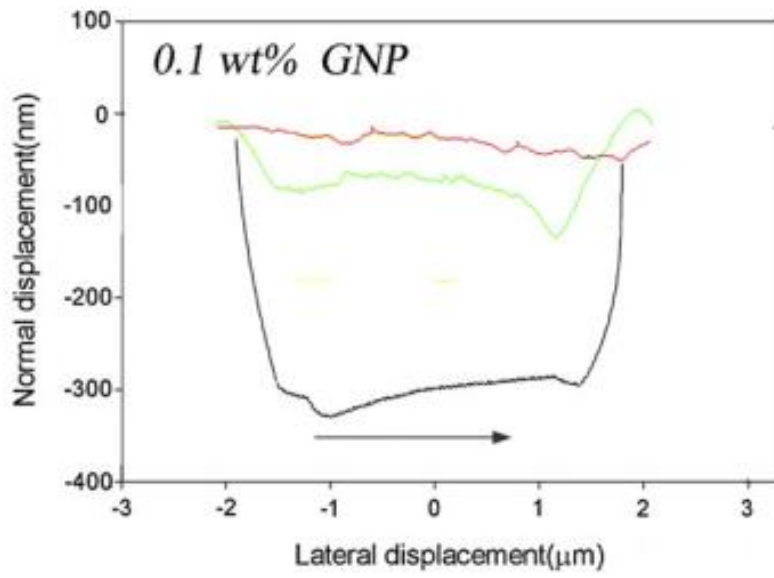


a)

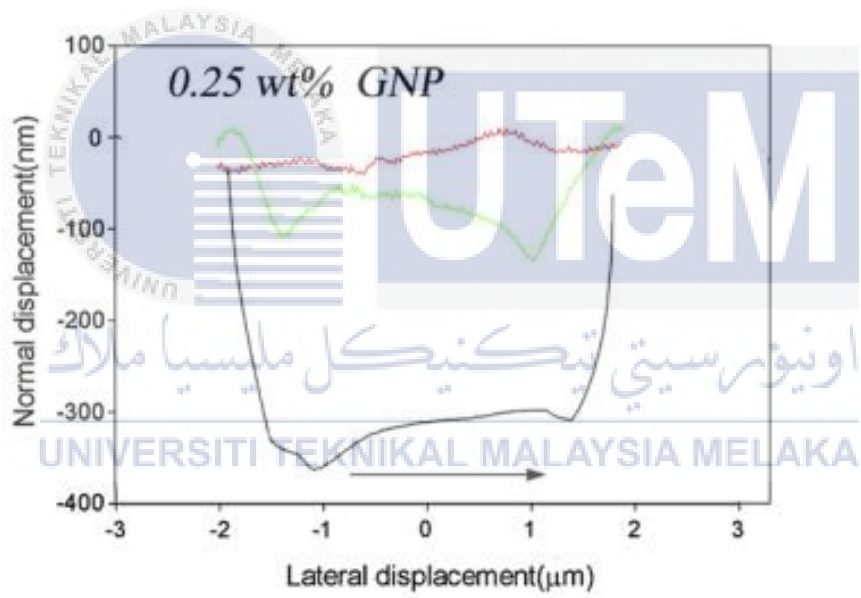


b)

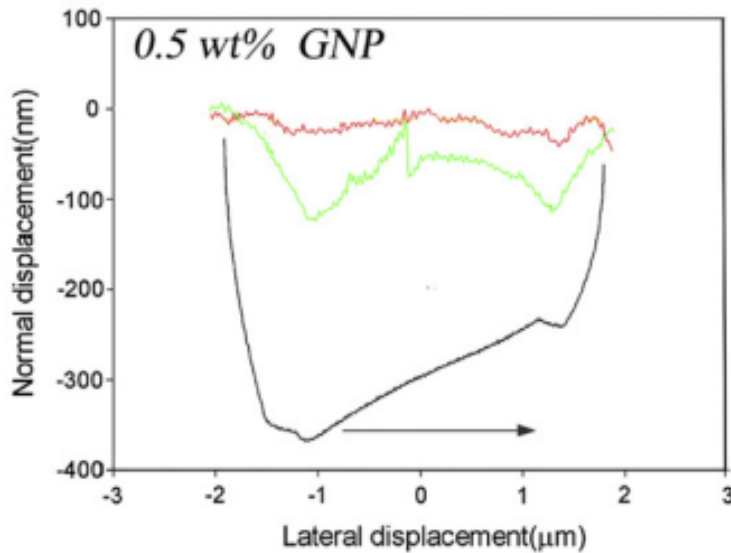




c)

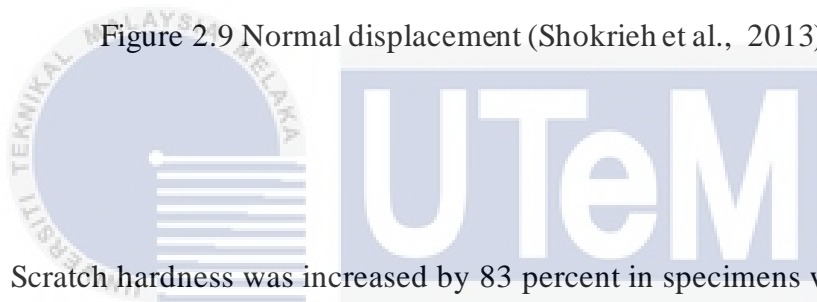


d)



e)

Figure 2.9 Normal displacement (Shokrieh et al., 2013)



Scratch hardness was increased by 83 percent in specimens with 0.5 wt.% GNP. At a load of 600 mN, this improvement in normal hardness was 50%. The Scratch hardness to normal hardness ratio is typically between 1.4 and 1.6. Other researchers have also observed higher scratch hardness values. Normal and scratch hardness is defined in the same way, i.e., the ability of a material to resist deformation, but the mechanisms involved are different.

In contrast to nano scratch hardness, which is primarily dynamic, typical indentation hardness is mostly quasi-static. A rigid indenter penetrates the specimen surface and slides along with it in the nano scratch test. As a result, the frictional resistance between the indenter and the material and lateral force is unavoidable. These factors do not exist in the nanoindentation test, and they are the primary cause of the difference between normal and scratch hardness.

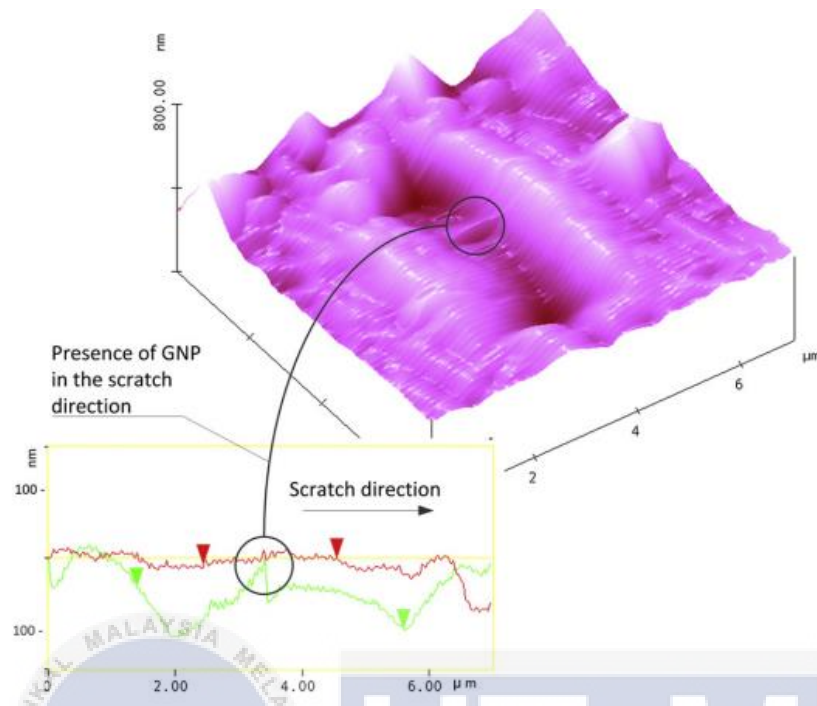


Figure 2.10 An AFM image from the scratch test on GNP-filled nanocomposites (Shokrieh et al., 2013)

As shown in **Fig. 2.10**, increasing the GNP content causes both scratch and hardness to increase similarly. However, the increase in scratch hardness is more significant than the increase in normal hardness between nanocomposites containing 0.25 and 0.5 wt.% of GNP, and the increase in normal hardness is smaller. It occurred due to the presence of graphene nanoplatelets in the direction of the nano-scratch test, which caused the scratch to occur (**Figure 2.11**). Depending on their direction of travel, the GNPs may be subjected to various loading conditions such as compression, bending, or buckling during this test. As a result, the indenter must exert more significant force to overcome these obstacles, and the scratch hardness will increase (Shokrieh et al., 2013).

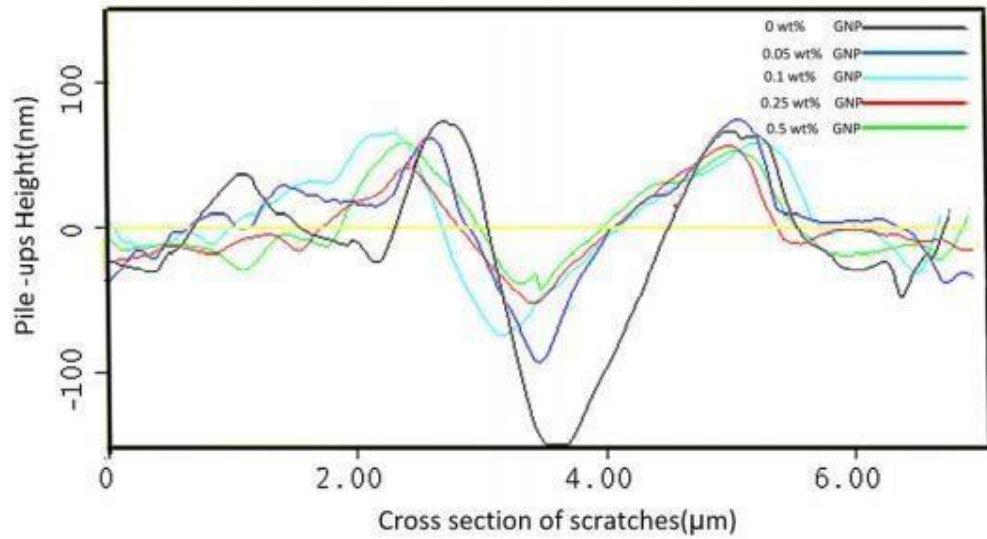


Figure 2.11 The cross-section scratch profiles of GNP-filled nanocomposites (Shokrieh et al., 2013)



## CHAPTER 3

### METHODOLOGY

#### 3.1 Overview

The detailed methodology for this research project includes the type of Graphene Nanoplatelets (GNP) 15  $\mu\text{m}$ , resin PEDOT PSS used and surfactant with are Dimethyl sulfoxide, mono ethylene glycol and Triton-X-100 the techniques for the SCI fabrication, the machine and apparatus used and the material characterization tests that are conducted on the SCI are described.

Below is a summary of the research activities involved in this project, as follows:

1. Designing the experimental process
2. Preparation of the procedures, variables and parameters of the experiment.
3. Listing of all the required standards for the related test.
4. Extract important material properties from the supplier datasheet for the specific Graphene Nanoplatelets (GNP), PEDOT: PSS and other chemicals used as filler.
5. Record formulation of the SCI based on past research and literature and the detailed steps involved during the processing route used to formulate the SCI.
6. Preparation of the specimens for mechanical and electrical tests.
7. Conduct electrical (four-point probe) to find the best formula on all sample to compare the effect of Graphene Nanoplatelets (GNP) aspect ratio in SCI.
8. A morphological study of the SCI using a Scanning Electron Microscope.

**Figure 3.1** show the summary of the methodology of this research from the start of the literature review study according to the research title till the final report writing to complete the project.

### 3.2 Flow Chart

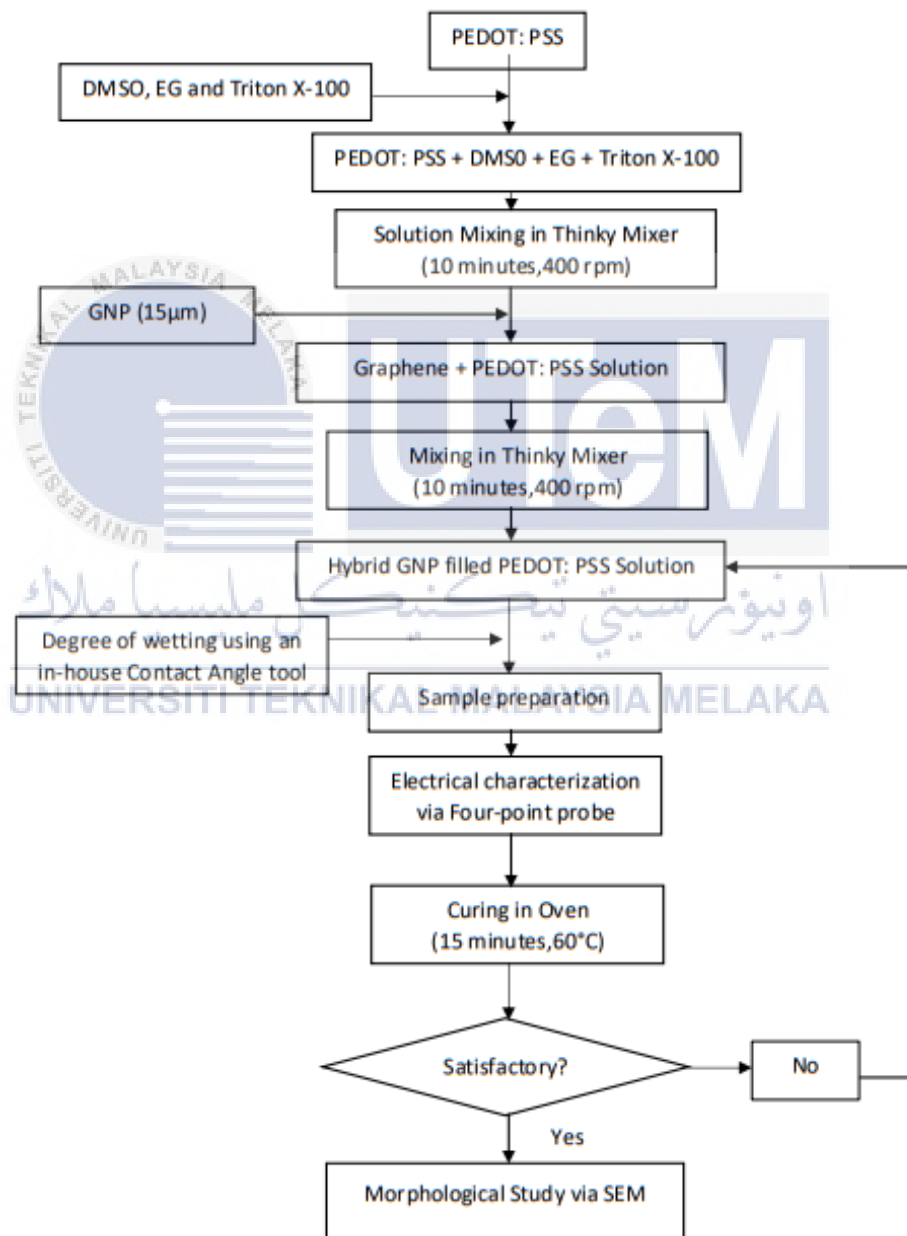


Figure 3.1 Flow chart of the methodology

### 3.3 Raw Materials

To formulate an electrically conductive adhesive, six parts of substances are needed. The first one is the polymer matrix of the SCI. In this research project, Poly(3,4-ethylene dioxythiophene) Polystyrene Sulfonate or PEDOT: PSS is chosen as the polymer matrix and must be mixed with surfactant or solvent with is Dimethyl sulfoxide, Mono ethylene glycol and Triton-X-100. The second part is the conductive filler added according to the filler loading, and in this research project, the specific particle size of the GNP used is 15  $\mu\text{m}$ .

#### 3.3.1 Polymer binder

In the SCI formulation for the SCI, PEDOT: PSS with 1.3 wt. % dispersion in  $\text{H}_2\text{O}$  (**Figure 3.2**), supplied by Sigma Aldrich, is used in this study. The chemical structure is given in Figure 3.3, while in **Table 3.1**, the material specification for PEDOT: PSS with 1.3 wt. % dispersion in  $\text{H}_2\text{O}$  is provided.



Figure 3.2 Sigma Aldrich PEDOT: PSS with 1.3 wt. % dispersion in the  $\text{H}_2\text{O}$  polymer binder

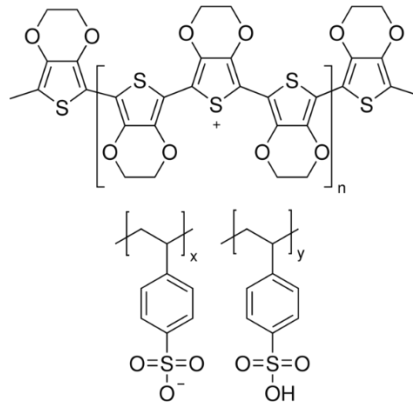


Figure 3.3 The chemical structure of Sigma Aldrich PEDOT: PSS with 1.3 wt. % dispersion in H<sub>2</sub>O polymer binder (SIGMA-ALDRICH, 2022c)

Table 3.1 Selected material specification for PEDOT: PSS with 1.3 wt. % dispersion in H<sub>2</sub>O (SIGMA-ALDRICH, 2022d)

| Criteria             | Specification                    |
|----------------------|----------------------------------|
| Product Number       | 768650                           |
| Colour               | Dark to very dark blue and black |
| Form                 | Paste                            |
| Residual Evaporation | 4-6%                             |
| Resistivity          | ≤130 ohm. sq                     |
| Viscosity            | ≥50000 mPa.s                     |
| Optical Density      | ≤20                              |



### 3.3.2 filler

Graphene nanoplatelets (GNP) with a particle size of 15  $\mu\text{m}$ , supplied from Sigma Aldrich, is used as the SCI conductive filler. **Table 3.2** lists the GNP material specification from the supplier's material datasheet.

Table 3.2 Specification of Graphene nanoplatelets conductive filler  
(SIGMA-ALDRICH, 2022b)

| Criteria       | Specification                 |
|----------------|-------------------------------|
| Product Number | 900420                        |
| Formula weight | 12.01 g/mol                   |
| Colour         | Dark Grey to Black            |
| Form           | Powder                        |
| Surface area   | 120-150 $\text{m}^2/\text{g}$ |
| Acid Content   | $\leq 0.5\%$                  |

### 3.3.3 Surfactant

A surfactant, also called a surface-active agent, is a substance like a detergent that makes it spread and wet more easily when added to a liquid. For example, surfactants are used in the dyeing of textiles to help the dye get into the fabric evenly. In addition, they are used to spread aqueous suspensions of dyes and perfumes that can't be dissolved in water. When a molecule is on the surface, it must be both hydrophilic (water-soluble) and lipophilic (oil-soluble) (soluble in lipids or oils).

Water and oil or lipids come together at the edges of bodies or droplets of each other to make them emulsify or foam (Britannica, 2020).

### 3.3.3.1 Dimethyl Sulfoxide (DMSO)

Dimethyl Sulfoxide (DMSO) is often employed in organic processes as a reaction medium and reagent. It may also be utilized as an oxidant in converting isonitriles to isocyanates. In addition, DMSO activated by oxalyl chloride can be employed as a catalyst in the oxidation of long-chain alcohols to carbonyls. In this study, the specific DMSO used is in a 250 g package with 99.9% purity, supplied by Mega Prima Niaga, Malaysia (Figure 3.4), while the chemical structure is given in Figure 3.5.



Figure 3.4 Dimethyl Sulfoxide (DMSO) used in this study

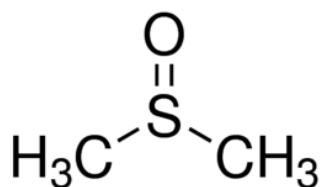


Figure 3.5 The chemical structure of Dimethyl Sulfoxide (DMSO) (SIGMA-ALDRICH, 2022a)

### 3.3.3.2 Mono Ethylene Glycol (MEG)

In most cases, this chemical called Mono Ethylene Glycol (MEG) is utilized for two purposes: as a raw material in producing polyester fibres and as an ingredient in antifreeze compositions. It is an odourless, colourless, sweet-tasting, poisonous, viscous liquid with no discernible flavour or colour. In this study, the specific MEG used is supplied by Eva Chem Malaysia (**Figure 3.6**). The physical and chemical properties are listed in Table 3.3.



Figure 3.6 Mono Ethylene Glycol (MEG) used in this study

Table 3.3 The physical and chemical properties of MEG used in this study

(Evacaely Enterprise Kofa Chemical Works (M) Sdn Bhd, n.d.)

| Description   | Property   |
|---------------|------------|
| Appearance    | Liquid     |
| Colour        | Colourless |
| Odour         | Mild sweet |
| Boiling Point | 197°C      |
| Flash Point   | 124°C      |

### 3.3.3.3 Triton-X-100

Triton X-100 is a well-known non-ionic surfactant and emulsifier that is frequently utilized. It is regarded as a relatively mild detergent that is non-denaturing, and it has been documented in multiple references as a commonly applied reagent. To remove protein and cellular organelles from cells, it is necessary to lyse them first. It can also be used to permeabilize the membrane of a live cell in preparation for transfection. Triton X-100 possesses homolytic properties and is employed to extract DNA from cells. In this study, the Triton X-100 used is supplied by R&M Chemicals with CAS no of 9002-93-1 (Figure 3.7). The chemical structure of this surfactant is given in Figure 3.8.



Figure 3.7 Triton X-100 used in this study

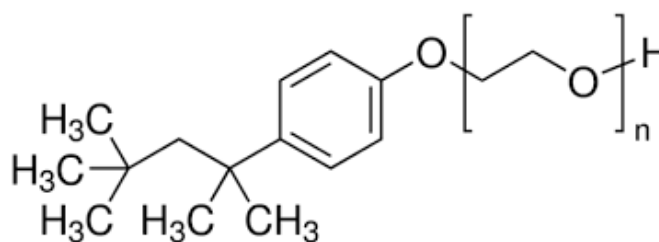


Figure 3.8 The Triton X-100 chemical structure (SIGMA-ALDRICH, 2022e)

### 3.4 Substrate

#### 3.4.1 Thermoplastic polyurethane (TPU)

Thermoplastic polyurethane or TPU is called the rubber-plastic bridge. The material appears rubber-like, making it highly flexible, durable and touch-smooth. TPU material consists of elastomers with good elasticity and stress resistance like abrasion and oil lubricants. Its structure consists of soft, hard, chain-linked segments. An example of the TPU chemical structure is shown in **Figure 3.9**. In this study, TPU is chosen as the substrate for the SCI, which features both flexible and stretchable properties. Takedo Sangyo supplies the TPU film with the specification listed in **Table 3.4**.

Table 3.4 Specification of the TPU substrate.

| Criteria            | TPU                                 |
|---------------------|-------------------------------------|
| Materials           | Thermoplastic polymer               |
| Physical Properties | A soft and stretchable polymer film |
| Supplier            | Takedo Sangyo                       |
| Grade               | Tough Grace-TG88-1                  |
| Thickness           | 100 $\mu\text{m}$                   |
| Appearance          | Transparent                         |
| Resistivity         | Dielectric                          |

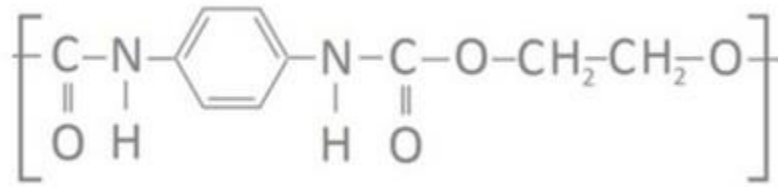


Figure 3.9 The chemical structure of Thermoplastic polyurethane (TPU)(mexpolímeros, 2021)

### 3.5 Formulation of SCI

This section presents the specific parametric study, specifically the process parameters investigated in establishing an optimum GNP-filled PEDOT: PSS SCI formulation.

#### 3.5.1 The GNP filled PEDOT: PSS Formulation

Table 3.5 gives the specific SCI formulation and specific processing parameters for the SCI formulation, which vary in mixing speed (rpm) and mixing time (minutes) using the centrifugal mixer, Thinky Mixer Model ARE-310. Here, the specific curing temperature and curing time in the oven set during the formulation is also reported. As shown in Table 3.5, the mixing time, speed and curing temperature with a varying GNP filler loading are investigated in this study. The effect of these processing parameters will be reported in Chapter 4 Results and Discussion regarding the SCI sheet resistance and contact angle before the optimum process parameters are identified and used for further characterization of the SCI formulated.

**Table 3.5** The GNP-filled PEDOT: PSS SCI formulation and process parameters considered in the study.

| Sample | SCI Mass (g) | GNP (wt.%) | GNP Mass (g) | PEDOT: PSS (wt.%) | PEDOT: PSS Mass (g) | Condition          |      |      |
|--------|--------------|------------|--------------|-------------------|---------------------|--------------------|------|------|
|        |              |            |              |                   |                     | 1                  | 2    |      |
|        |              |            |              |                   |                     | Mixing parameters  |      |      |
|        |              |            |              |                   |                     | Mixing Speed (rpm) | 2000 | 1500 |
|        |              |            |              |                   |                     | Mixing Time (min)  | 60   | 30   |
| 1      | 1.0          | 5          | 0.05         | 95                | 0.950               |                    |      |      |
| 2      | 1.0          | 10         | 0.10         | 90                | 0.900               |                    |      |      |
| 3      | 1.0          | 15         | 0.15         | 85                | 0.850               |                    |      |      |

Note (\*):

Curing temperature = 60°C and 100°C

Curing Time= 15 minutes

### 3.5.2 GNP- filled PEDOT: PSS and Surfactant Formulation

Initially, only PEDOT: PSS and GNP were used in this experiment, but when the ink was deposited onto the TPU, it felt brittle, and the ink was easily broken once cured. To overcome this problem, according to Chawarambwa et al. (2020), the addition of surfactant is added to make the ink adhere better onto the TPU substrate. However, it was observed that although the ink attached well to the TPU substrate, a notable amount of air entrapped in the form of a bubble was observed on the ink, as shown in **Figure 3.10**.



Figure 3.10 Bubble formation found following solution mixing of the SCI in which the PEDOT: PSS and GNP were mixed in a Thinky Mixer Machine

To overcome this issue, it was argued in the same literature that using a surfactant such as DMSO, MEG and Trito-x-100 and the use of a low-speed centrifugal mixer, that is, the Thinky Mixer at a mixing speed of 400 rpm for 10 minutes, was implemented, and the air bubble was successfully eliminated from the ink solution. The processing parameters used at this optimum formulation are given in **Table 3.6** in terms of the



Hybrid GNP-filled PEDOT: PSS formulation with varying GNP filler loading and the corresponding solvents used in the study (Seekaew et al., 2014) is given in **Table 3.7** respectively.

In addition, the detailed steps involved during SCI formulation and characterizations are shown in **Figure 3.11**. Here, upon successful completion of the solution mixing process, after curing of the SCI, the samples were left to be cooled down in room temperature condition for 24 hours before further characterization; these being the electrical using a four-point probe unit and Surface Morphology of GNP filled PEDOT: PSS: Surfactant using a Scanning Electron Microscope (SEM). The characterizations, which include both the qualitative (degree of wetting via contact angle measurement using an in-house tool) and quantitative analysis (electrical using a Four-point probe), is shown in **Figure 3.10**.

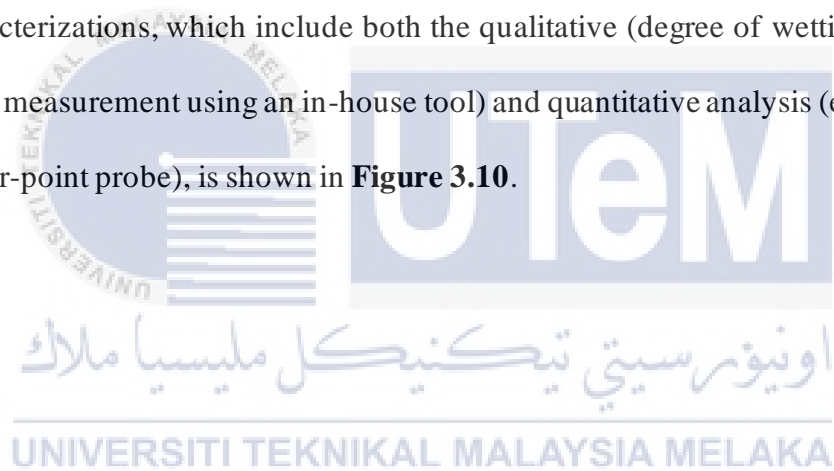


Table 3.5 Hybrid Graphene- PEDOT: PSS formulation for different filler and polymer loading.

| Sample | SCI<br>mass, g | Graphene<br>(wt.%) | Graphene<br>mass, g | PEDOT: PSS and<br>solvent<br>solution (wt.%) | PEDOT: PSS<br>Solution and<br>solvent<br>Mass, g | Substrates |
|--------|----------------|--------------------|---------------------|--|--|------------|
| 1      | 4              | 5                  | 0.2                 | 95   | 3.8  | TPU        |
| 2      | 4              | 7.5                | 0.3                 | 92.5   | 3.7  |            |
| 3      | 4              | 10                 | 0.4                 | 90   | 3.6  |            |

UNIVERSITI TEKNIKAL MALAYSIA MELAKA

Table 3.6 Detail information on the specific contents of the PEDOT: PSS polymer matrix and the solvents used in the study

(Seekaew et al., 2014)

| <b>PEDOT: PSS<br/>solution<br/>Mass, g</b> | <b>PEDOT: PSS<br/>(wt.%)</b> | <b>PEDOT: PSS<br/>Mass, g</b> | <b>DMSO<br/>(wt.%)</b> | <b>DMSO<br/>mass, g</b> | <b>EG<br/>(wt.%)</b> | <b>EG in<br/>mass, g</b> | <b>Triton x-<br/>100<br/>(wt.%)</b> | <b>Triton<br/>x—100<br/>(wt.%)</b> |
|--|------------------------------|-------------------------------|------------------------|-------------------------|----------------------|--------------------------|-------------------------------------|------------------------------------|
| 3.8  | 89.82                        | 3.413                         | 5.98                   | 0.2272                  | 3.99                 | 0.1516                   | 0.199                               | 0.00756                            |
| 3.7  | 89.82                        | 3.323                         | 5.98                   | 0.2213                  | 3.99                 | 0.1476                   | 0.199                               | 0.00736                            |
| 3.6  | 89.82                        | 3.234                         | 5.98                   | 0.2153                  | 3.99                 | 0.1436                   | 0.199                               | 0.00716                            |

Note (\*):

Curing temperature = 60°C and 100°C

Curing Time= 15 minutes

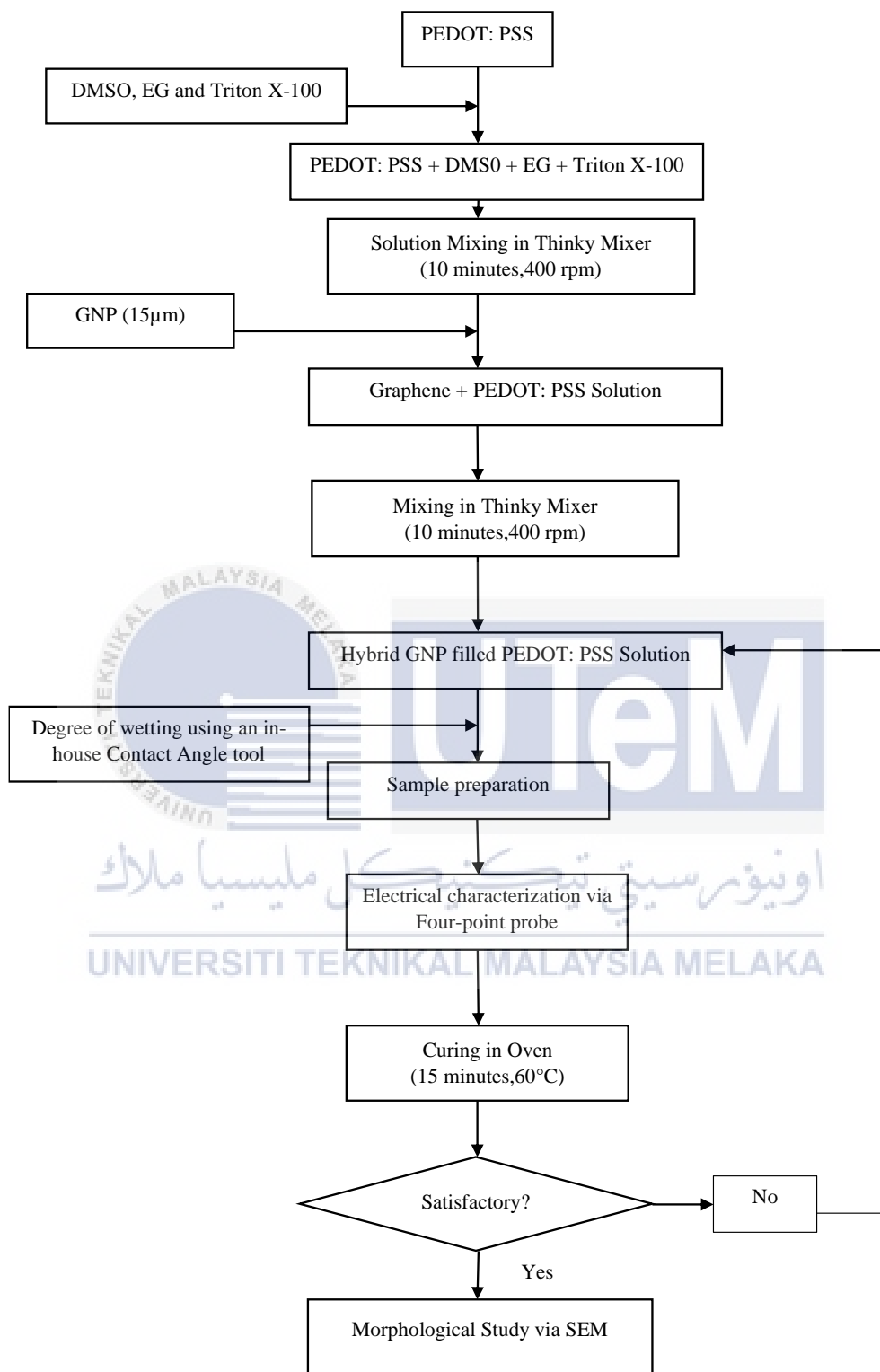


Figure 3.11 The steps in GNP-filled PEDOT: PSS SCI formulation and characterizations

### 3.6 Characterization of The SCI

As shown in **Figure 3.11**, the SCI characterizations include both the qualitative (degree of wetting via contact angle measurement using an in-house tool) and quantitative analysis (electrical using a Four-point probe) to attain the electrical performance of the SCI.

#### 3.6.1 Electrical Property Using a Four-Point Probe

After curing the SCI samples in the Memmert curing oven, they were taken out for cooling at room temperature. Then, the samples were inspected to observe whether they were satisfactory to proceed with the following process, in Stage 2 and Stage 3, respectively. If the sample is good, the next test is to test the electrical conductivity using a 4-point probe, as shown in **Figure 3.12**. A four-point probe is a device for determining the resistivity of samples. The substrate resistivity may be measured by providing a current through two external probes and the voltage via the inner probes.



Figure 3.12 A JANDEL In-Line Four-Point Probe

By testing the printed ECA resistivity, electrical conductivity can be analyzed and concluded. Resistivity test was conducted using JANDEL In-Line Four-Point Probe as shown in **Figure 3.13**, as per ASTM F390. An example of a printed SCI onto a TPU substrate based on the specified dimension is given in **Figure 3.13**.

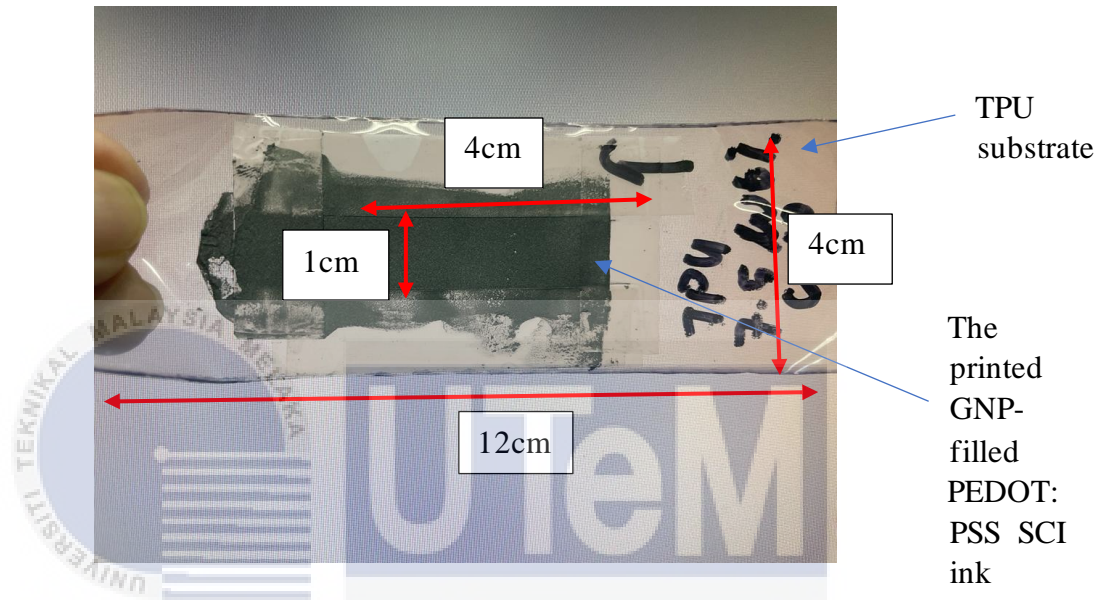


Figure 3.13 An example of the SCI printed onto a TPU substrate

The current flow through the probe was set at a specified ampere prior to the resistivity test. Then, each printed SCI were placed aligned and under a four-point probe head, and the probe head was lifted down until it touched the printed ECA. The sheet resistance calculation is expressed in Equation (3.1) as follows: -

$$R_s = G \cdot V_I \quad (3.1)$$

where  $R_s$  is sheet resistance ( $\Omega/\text{sq.}$ ),  $G$  is correction factor = 1.9475,  $V$  is voltage,  $I$  is input current.

The resistivity test was done at three positions (left, middle, right) of each printed SCI, and the resistivity results were recorded. They were averaged for each ECA with varying filler loading.

### 3.6.2 Bulk Resistivity of The SCI

In this study, in addition to the electrical characterization using a Four-point probe, a digital voltmeter was also used to evaluate the Bulk resistivity of the SCI. Here, the samples with dimensions of 4cm x 1 cm were prepared and measured in terms of resistivity using D03124-600V AC/ DC Auto-Ranging Digital Multimeter. The experimental setup is given in **Figure 3.14**.

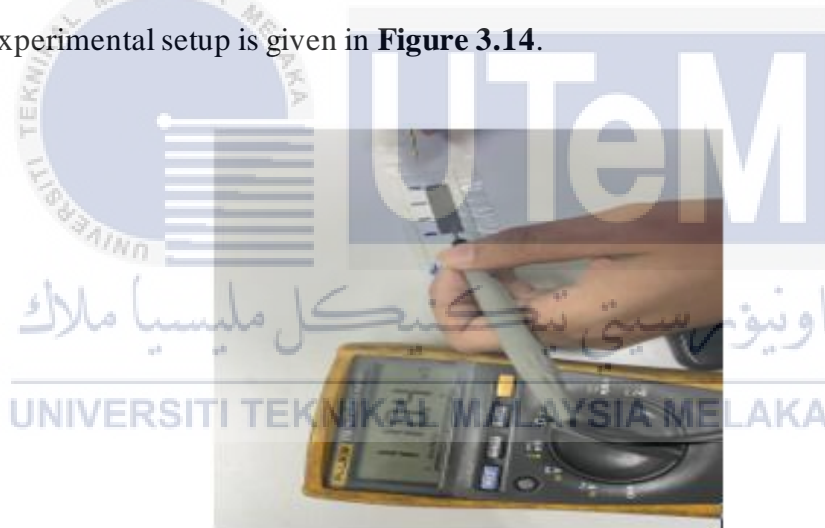


Figure 3.14 Experimental set up for the Bulk resistivity test on the SCI sample

### 3.6.3 Scanning Electron Microscope

Scanning Electron Microscope (SEM) is an imaging machine that operates using a focusing beam with high energy electrons to generate signals at the specimen surface is used for the surface morphological study. The air in the chamber may interfere with the scanning process; thus, the

inter-condition barrel was vacuumed. As a result, the focal length, level of magnification and brightness of the image need to be adjusted to obtain a better and more precise image.

In this final year project research work, an in-house Scanning Electron Microscope brand JEOL JSM-6010PLUS/LV model with an accelerated voltage of 5 kV was used in the Secondary electron images (SEI) mode. Before analysis, the existing test sample from the electrical test was cut to size and coated with a nonconductive substance to avoid charging by the electron beam.



Figure 3.15 A Scanning Electron Microscope from JEOL Model JSM-6010PLUS/LV

The morphological study via SEM is considered to study the effect of different filler loading and aspect ratio on SCI. The purpose of this analysis is to understand the GNP nanofiller distribution in the PEDOT: PSS matrix present in the SCI formulation.



## CHAPTER 4

### RESULTS AND DISCUSSION

#### 4.1 Introduction

This chapter presents the findings from the experimental work described in Chapter III Methodology. The results are aimed at achieving the study's objectives, which is to establish an optimized Graphene-PEDOT: PSS ink formulation using the best processing parameters identified through parametric study as well as looking into the effect of varying the GNP filler loadings on SCI electrical and mechanical performance using a TPU substrate, in terms of the sheet resistivity and adhesion strength of the SCI respectively.

The results attained from sheet resistance measurement of the SCI with varying GNP filler loading and mixing parameters subjected to a curing temperature of 60°C is presented in **Table 4.1**. The data shows the average sheet resistivity and corresponding conductivity using GNP with a filler size of 15  $\mu\text{m}$  and PEDOT: PSS.

The data found that the lowest conductivity is 5 wt.% graphene while the largest is 15 wt.%. In this case, PSS acts as an ionic dopant and an efficient dispersive agent for PEDOT. This polythiophene derivative is quite popular among conducting polymers because its electrical conductivity may be significantly improved by adding dopants such as sulphuric acid or formic acid or adjusting the volume ratio of PEDOT and PSS. The chemical role of PEDOT: PSS as a binder and dispersion was thoroughly investigated. Finally, a prototype of an all-printed, energy-efficient flexible heater was

created using the invented ink, and its heating efficiency was proved even after numerous bending cycles (Pillai et al., 2021).

## **4.2 Parametric Study Of The GNP-Filled PEDOT: PSS SCI Formulation**

### **4.2.1 Effect Of Processing Parameters (Mixing Time And Speed)**

This section presents and discusses the results attained from the SCI contact angle measurement with varying GNP filler loading and processing parameters. From the data presented in **Table 4.2**, it is apparent that increasing the mixing speed and mixing time affects the sheet resistivity of the ink and the corresponding contact angle, which is an indication of the wettability of the ink onto the TPU substrate. It is possibly because increasing GNP filler loading yields an increase in the SCI concentration, causing the contact angle to rise in response.

This finding is in good agreement with past literature in which it was argued that the higher the ink concentration, the greater the contact angle (Kim et al., 2011). In order to keep the ink concentration within a range suited for the electric function, the ink concentration must be adjusted. In addition, lower contact angles result in faster ink transfer rates than larger contact angles (Kang et al., 2009). The new ink's surface tension and contact angle are significantly reduced, implying that it may wet nearly any surface and make low-resolution patterns. During screen printing, a large shear force generated by the squeegee forces the ink to flow from the tensioned screen to the substrate (Pillai et al., 2021).

Table 4.1 The Sheet Resistivity and Conductivity of the SCI with varying GNP filler loading and mixing parameters

| Sample | GNP filler loading (wt.%) | Mixing Time | Mixing Speed | Average Sheet Resistivity ( $\Omega/\text{sq.}$ ) | Conductivity (S/m) |
|--------|---------------------------|-------------|--------------|---|--------------------|
| 1      | 5                         | 60          | 2000         | 23.368 $\pm$ 5.95                                 | 427.94             |
| 2      | 10                        | 60          | 2000         | 3.755 $\pm$ 0.64                                  | 2663.41            |
| 3      | 15                        | 60          | 2000         | 1.107 $\pm$ 1.20                                  | 9033.14            |
| 4      | 5                         | 30          | 1500         | 43.101 $\pm$ 17.49                                | 232.01             |
| 5      | 10                        | 30          | 1500         | 4.647 $\pm$ 1.94                                  | 2152.08            |
| 6      | 15                        | 30          | 1500         | 2.217 $\pm$ 0.81                                  | 4511.49            |

Table 4.2 The sheet resistivity and contact angle of the SCI with varying GNP filler loading and processing parameters

| Temperature | GNP filler loading<br>(wt.%) | Mixing Time<br>(minutes) | Mixing Speed<br>(rpm) | Sheet Resistivity<br>( $\Omega$ /sq.) | Conductivity<br>(S/m) | Contact Angle, $\theta$<br>( $^{\circ}$ ) |
|-------------|------------------------------|--------------------------|-----------------------|---------------------------------------|-----------------------|---|
| 60          | 5                            | 60                       | 2000                  | 23.37 $\pm$ 5.95                      | 427.94                | 69.8                                      |
|             | 10                           |                          |                       | 3.76 $\pm$ 0.64                       | 2663.41               | N/A                                       |
|             | 15                           |                          |                       | 1.11 $\pm$ 1.20                       | 9033.14               | N/A                                       |
|             | 5                            | 30                       | 1500                  | 43.10 $\pm$ 17.49                     | 232.01                | 69.25                                     |
|             | 10                           |                          |                       | 4.65 $\pm$ 1.94                       | 2152.08               | 66.77                                     |
|             | 15                           |                          |                       | 2.22 $\pm$ 0.81                       | 4511.49               | N/A                                       |
| 100         | 5                            | 60                       | 2000                  | 22.34 $\pm$ 8.94                      | 447.62                | 69.8                                      |
|             | 10                           |                          |                       | 5.79 $\pm$ 0.71                       | 1727.12               | N/A                                       |
|             | 15                           |                          |                       | 2.56 $\pm$ 0.49                       | 3906.25               | N/A                                       |
|             | 5                            | 30                       | 1500                  | 16.15 $\pm$ 3.58                      | 619.35                | 69.25                                     |
|             | 10                           |                          |                       | 6.90 $\pm$ 1.30                       | 1449.28               | 66.77                                     |
|             | 15                           |                          |                       | 2.24 $\pm$ 0.30                       | 4472.27               | N/A                                       |

Based on the preliminary results attained from the experimental work, it can be suggested that the mixing speed of 2000 rpm with a mixing time of 60 minutes using a curing temperature of 60°C shows the best processing parameters in formulating the GNP-filled PEDOT: PSS ink. The sheet resistivity of the SCI attained in this study from the different processing parameters with varying GNP filler loading is presented in **Figure 4.1**.

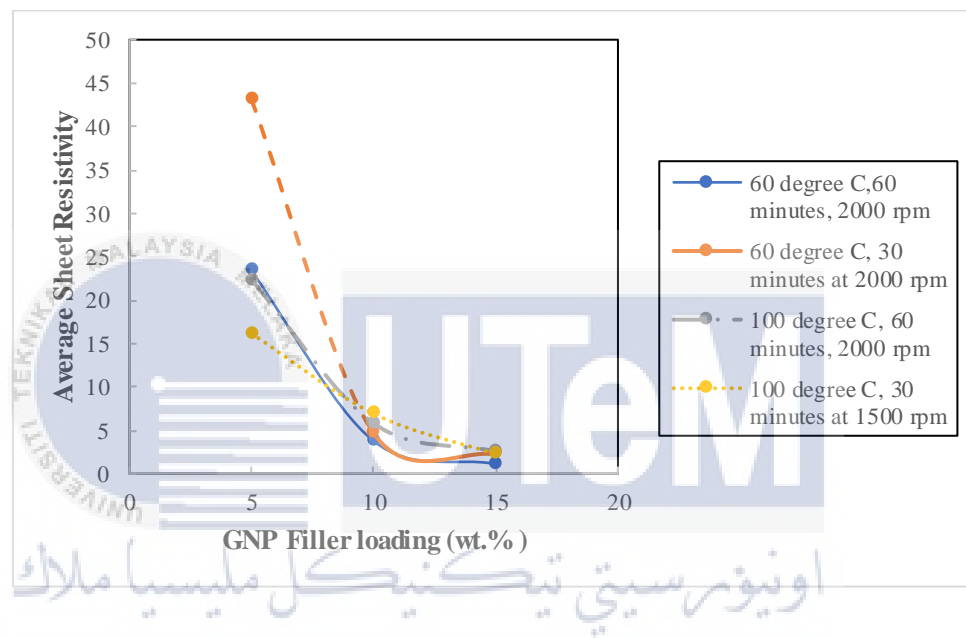


Figure 4. 1 The sheet resistivity of the SCI at specified processing parameters with varying GNP filler loading

#### 4.2.2 The Effect of Surfactant Used in GNPs And PEDOT: PSS Formulation

As discussed earlier in Section 3.5.2, the reason for the use of surfactant in the GNP-filled PEDOT: PSS SCI formulation is to overcome the issues of SCI brittleness when deposited onto the TPU substrate as well as the presence of air bubble. Therefore, the quantitative result from the processing route is presented and discussed in Section 4.2.

### 4.3 Effect of Mixing Speed and Mixing Time Of GNP Filled PEDOT: PSS With Surfactant

The results attained from sheet resistance measurement of the SCI with varying GNP filler loading and mixing parameters subjected to a curing temperature of 60°C is presented in **Table 4.3**. The data shows the average sheet resistivity and corresponding conductivity using GNP with filler size of 15µm and PEDOT: PSS at the optimum process parameters with a mixing time of 10 minutes at a mixing speed of 400 rpm. From the graph of average sheet resistivity vs GNP filler loading in **Figure 4.2**, it is apparent that the lowest conductivity is 5 wt.% graphene while the largest is 10 wt.%. PSS acts as an ionic dopant and an efficient dispersive agent for PEDOT in this case. This poly thiophene derivative is quite popular among conducting polymers because its electrical conductivity may be significantly improved by adding dopants such as sulphuric acid or formic acid or adjusting the volume ratio of PEDOT and PSS. The chemical role of PEDOT: PSS as a binder and dispersion was thoroughly investigated. Finally, a prototype of an all-printed, energy-efficient flexible heater was created using the invented ink, and its heating efficiency was proved even after numerous bending cycles (Pillai et al., 2021).

Table 4.3 Sheet Resistivity and Conductivity of the SCI with varying GNP filler loading and mixing parameters

| Sample | GNP filler loading (wt.%) | Mixing Time | Mixing Speed | Average Sheet Resistivity ( $\Omega/\text{sq.}$ ) | Conductivity (S/m) |
|--------|---------------------------|-------------|--------------|---|--------------------|
| 1      | 5                         | 10          | 400          | 9.90±1.37   | 1010.1             |
| 2      | 7.5                       | 10          | 400          | 5.82±0.96   | 1689.1             |
| 3      | 10                        | 10          | 400          | 3.97±0.46   | 2518.9             |

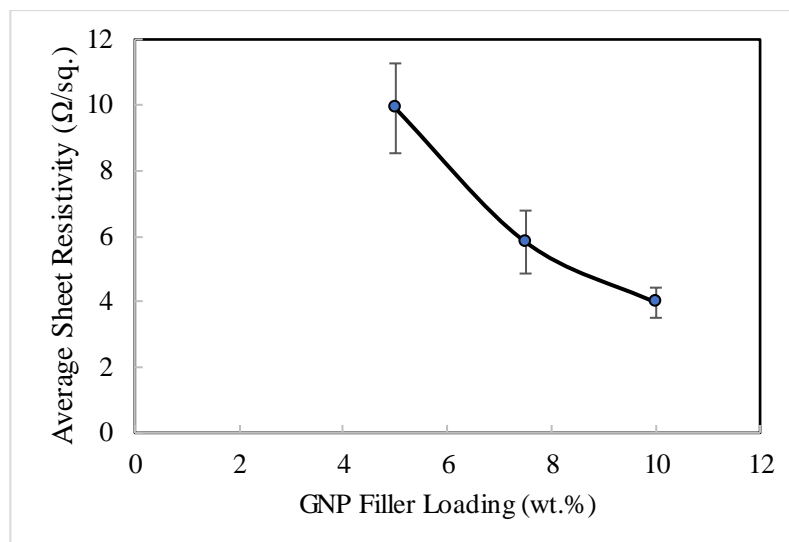


Figure 4.2 Sheet resistivity and the corresponding conductivity of the SCI with varying mixing parameters and GNP filler loading

#### 4.4 The Bulk Resistivity Test of GNP filled PEDOT: PSS Surfactant

In **Table 4.4**, the average Bulk resistivity of the SCI in which the surfactant was employed. With increasing GNP filler loading, from 5 to 10 wt.%, there is a 27% reduction in the average Bulk resistivity of the formulated GNP-filled PEDOT: PSS SCI. This trend is similar to those of the average sheet resistivity values reported using the four-point probe, with less accurate data attained due to the sensitivity of the equipment used.

Table 4.4 The Average Bulk Resistivity of the SCI (surfactant used)

| Sample | GNP filler loading (wt.%) | Mixing Time | Mixing Speed | Average Bulk Resistivity (Ω/sq.) |
|--------|---------------------------|-------------|--------------|----------------------------------|
| 1      | 5                         | 10          | 400          | 52.39±3.19                       |
| 2      | 7.5                       | 10          | 400          | 30.89±1.41                       |
| 3      | 10                        | 10          | 400          | 37.95±2.04                       |

#### 4.5 Surface Morphology of The GNP filled PEDOT: PSS: Surfactant SCI

As discussed in Section 3.6.3, the morphological study using SEM is presented in this chapter for selected SCI samples following the curing process. **Tables 4.5** and **4.6** presents the SEM micrograph showing the GNP filler distribution in PEDOT: PSS binder of the SCI with GNP filler loading of (a) 5 wt.%, (b) 7.5 wt.% and in (c) 10 wt.% (400 rpm and 10 minutes of mixing time) at a magnification of x200 and x1000x via SEI mode at 5 kV respectively.

As marked and labelled in the micrographs, evidence of void/pores are more apparent in the SCI with the lowest GNP filler loading, of 5 wt.%, as shown in Figure 4.5 and 4.6 (a). Furthermore, at increasing GNP filler loading of 7.5 wt.%, there appears to be better GNP filler distribution in the PEDOT: PSS matrix of the SCI system, with fewer traces of the pores/ voids formation, as given in Tables 4.5 and 4.6(b). Lastly, the highest GNP filler loading considered in this study is at 10 wt.% GNP, the surface appears to be more brittle-like, in Table 4.5 (c) with a magnification of x200, and a more precise observation can be attained in Table 4.6(c) at 1000x magnification.



Table 4.5 SEM micrograph showing the GNP filler distribution in PEDOT: PSS binder of the SCI with GNP filler loading of (a) 5 wt.%, (b) 7.5 wt.% and in (c) 10 wt.% (400 rpm and 10 minutes of mixing time) at a magnification of x200

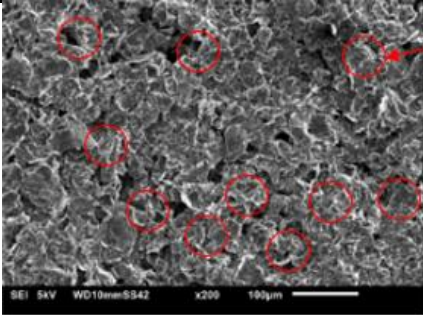
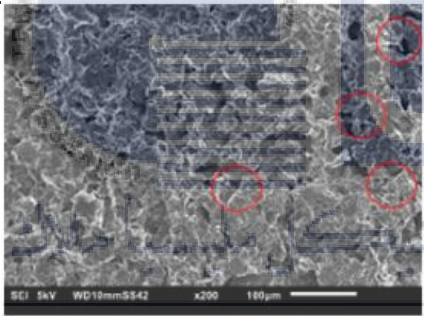
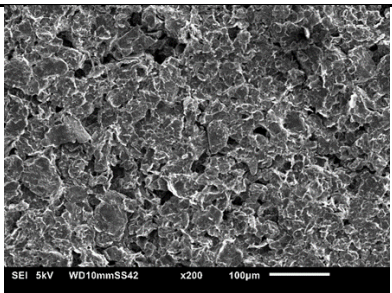
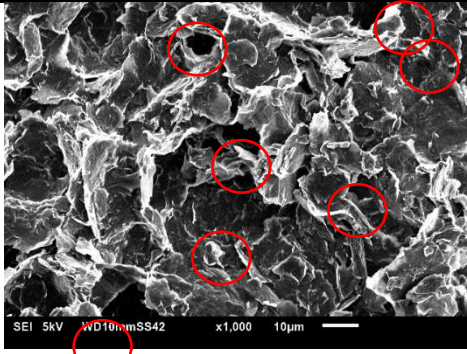
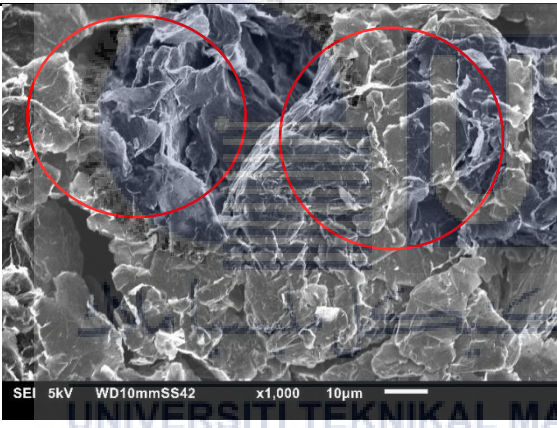
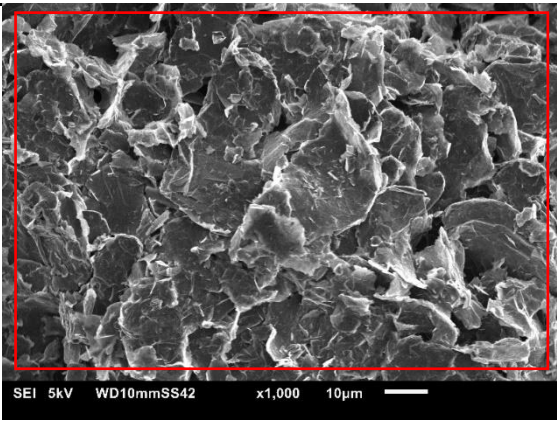
| SEM micrograph   | Remark  |
|--|---|
|  <p>(a) SCI filled with GNP filler loading of 5 wt.% (400 rpm and 10 minutes in centrifugal mixer)</p>    | <p>At 200x, traces of voids present in the SCI system, possibly due to the formation of a crack in the SCI, an indication of agglomeration of the GNP filler in the SCI system, with inhomogeneous filler distribution at 5 wt.% filler loading</p> |
|  <p>(b) SCI filled with GNP filler loading of 7.5 wt.% (400 rpm and 10 minutes in centrifugal mixer)</p> | <p>At 200x, there is a reduction of void present in the SCI, an indication of more efficient GNP filler distribution in the SCI system, at increasing GNP filler loading of 7.5 wt.%</p>  |
|  <p>(c) SCI filled with GNP filler loading of 10 wt.%</p>   | <p>At 200, evidence of a more brittle surface is observed, suggesting that the SCI has reached the threshold limit at increasing GNP filler loading of 10 wt.%</p>  |

Table 4.6 SEM micrograph showing the GNP filler distribution in PEDOT: PSS binder of the SCI with GNP filler loading of (a) 5 wt.%, (b) 7.5 wt.% and in (c) 10 wt.% (400 rpm and 10 minutes of mixing time) at a magnification of x1000

| SEM micrograph   | Remark   |
|--|--|
|  <p style="text-align: center;">(a)</p>   | <p>At 1000x, voids in the SCI system are more prominent.</p>   |
|  <p style="text-align: center;">(b)</p>  | <p>At 1000x, the SCI appears to show less presence of void with increasing GNP filler loading of 7.5 wt.%</p>  |
|  <p style="text-align: center;">(b)</p> | <p>At 1000x, more presence of the GNP is observed on the PEDOT: PSS matrix in the SCI system, exhibiting more brittleness on the surface, at increasing GNP filler loading of 10 wt.%.</p> |

## CHAPTER 5

### CONCLUSION AND RECOMMENDATION

#### 5.1 Conclusion

The effect of the processing parameters used during formulation of the GNP-filled PEDOT: PSS in which the GNP filler is varied between 5 to 10 wt.% and the ink was printed onto the TPU as a substrate was investigated in this study. The optimum process parameters were identified based on the SCI electrical properties and the qualitative aspect in terms of the ink deposition and degree of wetting via a contact angle measurement. Finally, the surface morphological study was done using a scanning electron microscope (SEM) and correlated with the results attained. 7.5wt.% is best because it has stable sheet resistance and bulk resistance values. Sem results show that figure 7.5.wt.% is very balanced and not clumped together.

In terms of electrical characterization, the sheet resistance of the SCI printed on TPU substrate reduces as the filler loading rises, suggesting high conductivity. Furthermore, the SCI printed on the TPU substrate has higher conductivity on the relatively higher GNP wt.%. However, one of the main challenges is that too much GNP causesglomeration and makes it impossible to generate a contact angle. It is because GNP is patchy in an ink region. According to the results, SCI with low viscosity is incompatible with the stencil printing process and affects the electrical characteristics of the printed SCI on the substrate.

Based on the findings of this study, it is possible to deduce that the SCI printed with varying GNP filler loading have a strong influence on the functional qualities of

the SCI. Furthermore, the surface quality of the SCI deposited onto the TPU substrates is critical in defining the SCI's superior electrical and mechanical characteristics, especially for applications such as wearable and flexible electronics.

## 5.2 Recommendation for Future Works

Stretchable conductive inks (SCI) have risen in popularity because of their great flexibility and expendability while maintaining outstanding conductivity. In addition, using carbon as conductive ink can save a significant amount of money. However, even though SCI has been utilized commercially, particularly carbon filler SCI, there are still areas for development to be studied to maximize the potential of a carbon filler.

The SCI formulation method shall be further improved to provide more homogenous distribution of the filler and epoxy in the SCI to minimize agglomeration of the graphene nanoplate, which reduces the SCI's reliability performance in superior electrical, mechanical characteristics SCI. Furthermore, a well-distributed graphene nanocarbon filler in SCI contributes to a large filler surface area accessible for absorbing a load from the polymer matrix. To address the issue, a mechanical stirrer shall be employed. Furthermore, a thorough study on the curing process and condition may be conducted since they play a crucial role in influencing the dependability of the SCI generated.

Furthermore, surface treatment of the polymer substrate can optimize the adhesion strength between SCI and the polymer substrate. It can improve adhesion by raising the surface tension of the polymer, altering its hydrophobicity, and expanding the surface contact area. Finally, the SCI printing method must be selected based on

the viscosity of the SCI, as the viscosity of the SCI and printing techniques are inextricably linked. For example, a 3D printing method could be considered to print the SCI.



## REFERENCES

Ashikin, A. A., Omar, G., Tamaldin, N., Nordin, M. A., & Akop, M. Z. (n.d.).

Electrothermal Effects of Stretchable Conductive Ink ( SCI ). 18–19.

Ashikin, A. S., Omar, G., Tamaldin, N., Kamarolzaman, A. A., Jasme, S., & Ani, F.

C. (2013). Comparative Study on the Polyethylene Terephthalate ( Pet ) and Thermoplastic Polyurethane ( Tpu ) As Substrate Materials for Conductive Ink. xx(January).

Kim, D. C., Shim, H. J., Lee, W., Koo, J. H., & Kim, D. H. (2020). Material-Based Approaches for the Fabrication of Stretchable Electronics. *Advanced Materials*, 32(15), 1–29. <https://doi.org/10.1002/adma.201902743>

Merilampi, S., Laine-Ma, T., & Ruuskanen, P. (2009). The characterization of electrically conductive silver ink patterns on flexible substrates. *Microelectronics Reliability*, 49(7), 782–790. <https://doi.org/10.1016/j.microrel.2009.04.004>

Barkoula, N. M., Alcock, B., Cabrera, N. O., & Peijs, T. (2008). Flame-Retardancy Properties of Intumescent Ammonium Poly(Phosphate) and Mineral Filler Magnesium Hydroxide in Combination with Graphene. *Polymers and Polymer Composites*, 16(2), 101–113. <https://doi.org/10.1002/pc>

Ham, H. A. Q. P., Chemical, D., Arks, M. A. J. M., & Chemical, D. (2012). Epoxy Resins. <https://doi.org/10.1002/14356007.a09>

Kim, J., Oh, J., Lee, K. Y., Jung, I., & Park, M. (2017). Dispersion of graphene-based nanocarbon fillers in polyamide 66 by dry processing and its effect on mechanical properties. *Composites Part B: Engineering*, 114, 445–456. <https://doi.org/10.1016/j.compositesb.2017.01.054>

Mendez-Rossal, H. R., & Wallner, G. M. (2019). Printability and properties of conductive inks on primer-coated surfaces. *International Journal of Polymer Science*, 2019. <https://doi.org/10.1155/2019/3874181>

Rao, C. N. R., Biswas, K., Subrahmanyam, K. S., & Govindaraj, A. (2009). Graphene, the new nanocarbon. *Journal of Materials Chemistry*, 19(17), 2457–2469. <https://doi.org/10.1039/b815239j>

Shokrieh, M. M., Hosseinkhani, M. R., Naimi-Jamal, M. R., & Tourani, H. (2013). Nanoindentation and nanoscratch investigations on graphene-based nanocomposites.

*Polymer Testing*, 32(1), 45–51. <https://doi.org/10.1016/j.polymertesting.2012.09.001> Yang, Y., Deng, H., & Fu, Q. (2020). Recent progress on PEDOT:PSS based polymer blends and composites for flexible electronics and thermoelectric devices. *Materials Chemistry Frontiers*, 4(11), 3130–3152. <https://doi.org/10.1039/d0qm00308e>

Barkoula, N. M., Alcock, B., Cabrera, N. O., & Peijs, T. (2008). Flame-Retardancy Properties of Intumescent Ammonium Poly(Phosphate) and Mineral Filler Magnesium Hydroxide in Combination with Graphene. *Polymers and Polymer Composites*, 16(2), 101–113. <https://doi.org/10.1002/pc>

Ashikin, A. S., Omar, G., Tamaldin, N., Jasmee, S., Hamid, H. A., Jalar, A., & Che Ani, F. (2020). Thermo-mechanical and adhesion performance of silver-filled conductive polymer composite (SFCP) using thermoplastic polyurethane (TPU) substrate. *International Journal of Nanoelectronics and Materials*, 13(Special Issue ISSSTE 2019), 419–430.

Ashikin, A. S., Omar, G., Tamaldin, N., Kamarolzaman, A. A., Jasmee, S., & Ani, F. C. (2013). *Comparative Study on the Polyethylene Terephthalate ( Pet ) and Thermoplastic Polyurethane ( Tpu ) As Substrate Materials for Conductive Ink.* xx(January).

Britannica. (2020). *Surfactant Chemical Compound*. T. Editors of Encyclopaedia. <https://www.britannica.com/science/surfactant>

El-Aila, H. J. Y. (2009). Interaction of nonionic surfactant Triton-X-100 with ionic surfactants. *Journal of Dispersion Science and Technology*, 30(9), 1277–1280. <https://doi.org/10.1080/01932690902735207>

*Evacaely Enterprise Kofa Chemical Works (M) Sdn Bhd. (n.d.). M.*

Garcia-Chavez, L. Y., Schuur, B., & De Haan, A. B. (2012). Liquid-liquid equilibrium data for mono ethylene glycol extraction from water with the new ionic tetraoctyl ammonium 2-methyl-1-naphtoate as solvent. *Journal of Chemical Thermodynamics*, 51, 165–171. <https://doi.org/10.1016/j.jct.2012.03.009>



Htwe, Y. Z. N., Abdullah, M. K., & Mariatti, M. (2021). Optimization of graphene conductive ink using solvent exchange techniques for flexible electronics applications. *Synthetic Metals*, 274(January), 116719. <https://doi.org/10.1016/j.synthmet.2021.116719>

Merilampi, S., Laine-Ma, T., & Ruuskanen, P. (2009). The characterization of electrically conductive silver ink patterns on flexible substrates. *Microelectronics Reliability*, 49(7), 782–790. <https://doi.org/10.1016/j.microrel.2009.04.004>

mexpolímeros. (2021). *Polyurethane thermoplastic TPU*. <https://www.mexpolimeros.com/eng/tpu-1.html>

Nguyen, T. N. H., Nolan, J. K., Cheng, X., Park, H., Wang, Y., Lam, S., Lee, H., Kim, S. J., Shi, R., Chubykin, A. A., & Lee, H. (2020). Fabrication and ex vivo evaluation of activated carbon–Pt microparticle based glutamate biosensor. *Journal of Electroanalytical Chemistry*, 866, 114136. <https://doi.org/10.1016/j.jelechem.2020.114136>

Notman, R., Noro, M., O'Malley, B., & Anwar, J. (2006). Molecular basis for dimethylsulfoxide (DMSO) action on lipid membranes. *Journal of the American Chemical Society*, 128(43), 13982–13983. <https://doi.org/10.1021/ja063363t>

Raheem. (2018). *The Effect of Carbon NanoTube Aspect Ratio on The Functional Properties of Electrically Conductive Adhesives*. 77.

SIGMA-ALDRICH. (2022a). *Dimethyl sulfoxide*.  
<https://www.sigmaaldrich.com/MY/en/product/sigma/d2650>

SIGMA-ALDRICH. (2022b). *Graphene nanoplatelets*.  
<https://www.sigmaaldrich.com/MY/en/product/aldrich/900420>

SIGMA-ALDRICH. (2022c). *Poly(3,4-ethylenedioxythiophene)-poly(styrenesulfonate)*.  
<https://www.sigmaaldrich.com/MY/en/product/aldrich/483095>

SIGMA-ALDRICH. (2022d). *Poly(3,4-ethylenedioxythiophene)-poly(styrenesulfonate)*.  
<https://www.sigmaaldrich.com/MY/en/product/aldrich/483095>

SIGMA-ALDRICH. (2022e). *Triton<sup>TM</sup> X-100*.  
<https://www.sigmaaldrich.com/MY/en/product/mm/648462>

Wan Abdul Rahman, W. A. (2017). *the Effect of Substrate Surface Conditions on Mechanical Performance of*.

Yang, Y., Deng, H., & Fu, Q. (2020). Recent progress on PEDOT:PSS based polymer blends and composites for flexible electronics and thermoelectric devices. *Materials Chemistry Frontiers*, 4(11), 3130–3152. <https://doi.org/10.1039/d0qm00308e>